This article has been accepted for inclusion in a future issue of this journal. Content is final as presented, with the exception of pagination.

The Piezoresistive Effect of SiC for MEMS Sensors at High Temperatures: A Review

Hoang-Phuong Phan, Dzung Viet Dao, Koichi Nakamura, Sima Dimitrijev, *Senior Member, IEEE*, and Nam-Trung Nguyen

***Abstract*— Silicon carbide (SiC) is one of the most promising materials for applications in harsh environments thanks to its excellent electrical, mechanical, and chemical properties. The piezoresistive effect of SiC has recently attracted a great deal of interest for sensing devices in hostile conditions. This paper reviews the piezoresistive effect of SiC for mechanical sensors used at elevated temperatures. We present experimental results of the gauge factors obtained for various poly-types of SiC films and SiC nanowires, the related theoretical analysis, and an overview on the development of SiC piezoresistive transducers. The review also discusses the current issues and the potential applications of the piezoresistive effect in SiC. [2015-0092]**

***Index Terms*— Silicon carbide, piezoresistive effect, piezoresistance, harsh environments, microelectromechanical systems (MEMS).**

I. Introduction

DISCOVERED by Smith in 1954, the piezoresistive effect in semiconductors has been intensively and relentlessly investigated for more than five decades [1]. The piezoresistive effect has also been applied in various Micro Electro Mechanical Systems (MEMS) sensors, utilizing its advantages such as device miniaturization, low power consumption and simple readout circuit [2], [3], over other sensing mechanisms (optical, electro static, piezoelectric). Among various semiconductors, silicon is the most favorable material for developing piezoresistance based devices thanks to its large magnitude of effect, worldwide availability, and mature fabrication technologies [4]–[6]. Common applications employing the piezoresistance of Si can be found in inertia, pressure, tactile and bio sensors which operate at room temperature [7]–[11].

In industries involving fuel combustion, such as aerospace and automotive systems, there is a great demand for monitoring pressure inside the engine chambers at high temperatures. Monitoring pressure and temperature can be utilized to diagnose the performance of engines, and thus could improve the efficiency of the combustion process [12]. In addition, the measurement of the mechanical strain in hot sections of turbines is also vital to the prediction of the failure of engines [13]. Therefore, it is increasingly important to develop mechanical sensing devices which can withstand hostile conditions such as high temperatures and increased corrosion [14]–[16]. Silicon is not a suitable material for such conditions because of its relatively low energy gap (1.12 eV), which limits its piezoresistive applications below 200 °C [17], [18]. Consequently, the piezoresistive effect in materials with a large energy gap (e.g. gallium nitride (GaN), silicon carbide (SiC)) is of interest for mechanical sensors at elevated temperatures (Fig. 1) [14], [19]. Among several large band gap materials, SiC is one of the most promising semiconductors for MEMS transducers used in harsh environments due to its large energy band gap of 2.3 to 3.4 eV, excellent chemical inertness, and large Young's modulus [20], [21]. The rapid growth of the

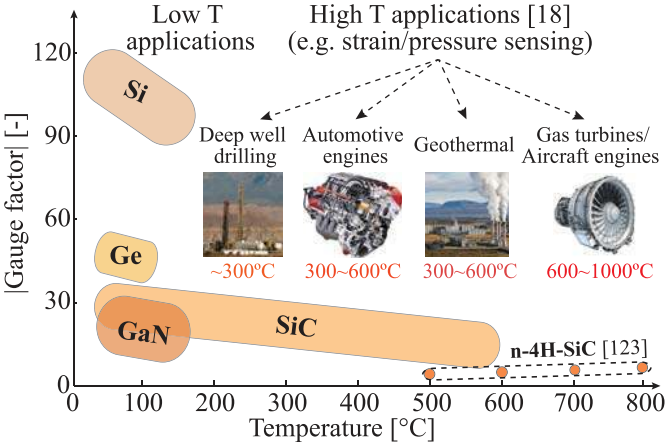

Fig. 1. The piezoresistive effect in common semiconductors. The piezoresistive effect of Si is favorable for low-temperature applications, such as inertial sensors, pressure sensors, strain gauges, and cantilever sensors, operated below 200 °C. Silicon carbide [68], gallium nitride (GaN) [27], [28], on the other hand, are good candidates for devices operated at high temperatures and harsh environments such as turbine engines, deep well-drilling, and spacecrafts [12]. To date, the maximum temperature at which the piezoresistance of GaN has been reported is below 200 °C [28]. On the other hand, for SiC, the highest characterized temperature is 800 °C, in which the gauge factors increased when increasing temperatures from 500 to 800 °C [123]. Okojie *et al.* assumed that packaging may contribute to the increase in the gauge factors of n-type 4H-SiC, and "the mechanism responsible for this phenomenon and the hypotheses proposed are being investigated". (Note that the gauge factors in [123] are bridge gauge factors, not longitudinal or transverse gauge factors.)

Manuscript received April 1, 2015; revised July 31, 2015; accepted August 13, 2015. Subject Editor R. Maboudian. *(Corresponding author: Hoang-Phuong Phan.)*

H.-P. Phan, D. V. Dao, S. Dimitrijev, and N.-T. Nguyen are with the Queensland Micro- and Nanotechnology Centre, Griffith University, Nathan, QLD 4111, Australia (e-mail: hoangphuong.phan@griffithuni.edu.au; d.dao@griffith.edu.au; s.dimitrijev@griffith.edu.au; nam-trung.nguyen@griffith.edu.au).

K. Nakamura is with the Center for the Promotion of Interdisciplinary Education and Research, Kyoto University, Kyoto 606-8501 Japan, and also with the Department of Materials Science and Engineering, Egypt–Japan University of Science and Technology, Alexandria 21934, Egypt (e-mail: koichi@cpier.kyoto-u.ac.jp).

Color versions of one or more of the figures in this paper are available online at http://ieeexplore.ieee.org.

Digital Object Identifier 10.1109/JMEMS.2015.2470132

1057-7157 © 2015 IEEE. Personal use is permitted, but republication/redistribution requires IEEE permission.
See http://www.ieee.org/publications_standards/publications/rights/index.html for more information.

This article has been accepted for inclusion in a future issue of this journal. Content is final as presented, with the exception of pagination.

TABLE I
PROPERTIES OF SiC AND OTHER MATERIALS

Properties	SiC	Si	Diamond	GaN
Energy gap (eV) [20], [31]	2.3 (3C-SiC) to 3.4 (2H-SiC)	1.12	5.5	3.4
Breakdown voltage (V/cm) [20], [48]	4×10^6	3 to 6×10^5	10×10^6	3×10^6
Electron mobility (cm^2/Vs) [20], [48]	1000	1500	2200	900
Hole mobility (cm^2/Vs) [20], [48]	40 to 100	100 to 500	1600	150
Young's modulus (GPa) [31], [38]	300 to 500	130 to 180	1000	200 to 300
Melting point (°C) [20], [31]	2830*	1410	1400**	2400
Thermal conductivity ($Wcm^{-1}K^{-1}$) [15], [31]	5	1.5	20	1.3
Chemical Inertness [15]	Excellent	Poor	Good but burn	Good
MEMS compatibility [15]	Good	Excellent	Poor	Fair
Availability/Cost [15]	Fair	Excellent	Poor	Fair

* sublimation temperature [20]
** phase change temperature [20]

SiC market [22], the availability of large-scale commercial SiC wafers [23], [24], and advanced MEMS technologies [25] also offer SiC a great advantage over other large band gap materials.

The piezoresistive effect in SiC has been studied for more than two decades, both theoretically and experimentally, along with the development of various SiC piezoresistive sensors operated at 800 °C [68]–[73]. To the best of our knowledge, there are only a few articles reviewing the piezoresistive effect of SiC to date. In the review of piezoresistance in semiconductors of Barlian *et al.* [1], the piezoresistive effect in 3C-SiC was mentioned but not discussed in detail. Werner *et al.* reviewed some preliminary experimental results on the characterization of the piezoresistance in 3C and 6H-SiC in the 1990s [14]. However, the effect in other poly types such as 4H-SiC, amorphous SiC, and SiC nanowires was not reported. The influence of parameters including orientation dependence and doping concentration, as well as theoretical studies, were also omitted. Additionally, a report on the recent development of SiC piezoresistive sensors was not presented in the review paper of Werner *et al.*

This paper reviews the piezoresistive effect in SiC for MEMS transducers, covering both experimental and theoretical studies, and provides important information for MEMS designers on the effects of crystal defects, orientation dependence, carrier-concentration dependence as well as temperature dependence. Applications based on the piezoresistive effect in SiC are also presented. Lastly, the current issues and perspectives for further study and applications of the piezoresistive effect in SiC are also discussed.

II. SILICON CARBIDE MATERIAL

A. Properties of Silicon Carbide Material

Silicon carbide occurs in three states: single crystalline, polycrystalline, and amorphous. Crystalline SiC consists of covalent bonds between Si and C atoms which form tetrahedrons. Silicon carbide exhibits a one-dimensional polymorphism, resulting in different poly-types which are differentiated from each other by the stacking sequence of each tetrahedral bonded Si-C bilayer [29]. There are more than 200 poly-types which are categorized into either α-SiC or β-SiC. β-SiC, commonly known as 3C-SiC, is the only cubic crystalline structure of SiC, whereas 2H-SiC, 4H-SiC, and 6H-SiC are the most common poly-types of α-SiC [30]. Table I lists the properties of the most common single crystalline SiC poly-types (3C-SiC, 4H-SiC, and 6H-SiC) in comparison to Si, the conventional MEMS material, and other wide energy gap materials such as diamond and GaN [20], [31], [32]. Advantages of SiC include the wide energy gap that varies from 2.3 eV in 3C-SiC to 3.4 eV in 2H-SiC, high carrier mobilities and high breakdown voltage which are all desirable properties for high-temperature and high-power applications [33], [34].

Silicon carbide is suitable for high temperature applications, not only due to its large energy gap, but also due to its high melting point of above 2500 °C and high thermal conductivity of 5 $Wcm^{-1}K^{-1}$. Utilizing the advantages of rapid heating and cooling, various SiC-based micro heaters and mass flow sensors have been developed [35]–[37].

Silicon carbide is also well known for its excellent mechanical properties. With a high hardness of 9.15 (compared to 10.0 of diamond) and excellent wear resistance, SiC has been used as a coating layer in micromachined devices in order to prevent erosion [20]. Compared to Si, SiC has a higher Young's modulus (about 2 to 5 times) [38], [39] and a comparable density; therefore, SiC is also preferable in high frequency resonators/vibrators [40] since the larger ratio of Young's modulus to mass density could enhance the resonance frequency of MEMS devices. As such, utilizing these superior mechanical properties, SiC based resonators with a Q factor of up to 1 million and a high frequency up to several GHz were developed [41], [42]. Reviews of SiC based resonators are available elsewhere [43].

Furthermore, the excellent properties of SiC make it a versatile material for bio applications [44]. With its transmission of visible light and absorption of UV wavelengths, SiC is an ideal material for optical bio-sensing devices. With chemical inertness and high corrosion resistance, SiC based transducers are suitable for complex environments such as body fluid. Its large

This article has been accepted for inclusion in a future issue of this journal. Content is final as presented, with the exception of pagination.

Young's modulus and low friction coefficients make SiC an ideal material for smart implants and *in vivo* biosensors [45]. As such, Gabriel *et al.* developed a 6H-SiC based micro-needle, which was used for tissue monitoring during clinical organ transplantation. The 6H-SiC needle outperformed the Si-based needle, both in terms of mechanical response with a four times higher modulus of rupture, and electrical measurement with a 10-fold extended frequency range [46]. For further reading on the compatibility of SiC for bio-MEMS applications, we recommend the review of Oliveros *et al.* [44].

Besides SiC, there are various large band gap materials such as III nitride (e.g. GaN, AlN), diamond like carbon (DLC), and zinc selenide (ZnSe) [30], [47], [48]. Silicon carbide possesses several advantages over other wide band gap semiconductors, including the availability of native substrates and advanced MEMS processing inherited from Si technologies [49], [50]. In addition, compared to other common large band gap materials such as gallium nitride and aluminum nitride, silicon carbide has significantly lower crystal dislocations [16], [18]. For the above-mentioned reasons, it is understandable that more research has been carried out for SiC than other wide band gap materials for high temperature applications [16], [51].

III. Piezoresistive Effect of Silicon Carbide

This section describes the definition of the piezoresistive effect and the gauge factors of several SiC poly-type films and nanowires. Typical applications of the piezoresistive effect in SiC are also presented. A description of the piezoresistive effect in other materials, particularly in Si, can be found in the review of Barlian *et al.* [1].

A. Piezoresistive Effect in Semiconductors

The piezoresistive effect is defined as the change of electrical resistance under mechanical stress or strain. Denoting the resistivity, length, width and thickness of a resistor by ρ, l, w and t, respectively, its resistance is given by:

$$R = \rho \frac{l}{wt} \tag{1}$$

Under an applied strain, the dimensions of the resistor and its resistivity change, resulting in the change of the resistance:

$$\frac{\Delta R}{R} = \frac{\Delta \rho}{\rho} + \frac{\Delta l}{l} - \frac{\Delta w}{w} - \frac{\Delta t}{t} = \frac{\Delta \rho}{\rho} + (1 + 2\gamma)\varepsilon \tag{2}$$

where $\varepsilon = \Delta l / l$ is the strain in the longitudinal orientation and γ is the Poisson's ratio of the material. The piezoresistive effect is commonly quantified by the gauge factor, which is defined as the fractional change in the resistance per unit strain:

$$GF = \frac{\Delta R/R}{\varepsilon} = \frac{\Delta \rho/\rho}{\varepsilon} + (1 + 2\gamma) \tag{3}$$

In most metals the resistivity remains almost constant when stress is applied, hence the gauge factor mainly depends on the mechanical properties of the metals and varies between 0 and 2 [52]. On the other hand, in semiconductors such as Si, SiC, and DLC, the applied stress/strain alters the carrier density and mobility, leading to a significant change of the resistivity or conductivity [1]. In this review, we use gauge factor (GF) as the parameter to evaluate and compare the magnitude of the piezoresistive effect in SiC poly types.

TABLE II
Index Transformation Scheme

Tensor notation	11	22	33	23 & 32	13 & 31	12 & 21
Matrix notation	1	2	3	4	5	6

The relative change of resistivity ($\Delta\rho/\rho$) can also be presented as a function of the applied stress (σ), using a parameter named piezoresistive coefficient (π): $\Delta\rho/\rho = \pi\sigma$. When a uniaxial stress is applied, the stress is connected to the strain via Hooke's law: $\sigma = E\varepsilon$, where E is the Young's modulus of SiC. Thus, the relationship between the gauge factor and the piezoresistive coefficient is $GF = E\pi$ [1]. In the general case, the change of resistivity $\Delta\rho_{ij}$ is a second rank tensor, which is connected to stress tensors (σ_{kl}) by a forth-rank piezoresistive coefficient tensor (π_{ijkl}) [55]:

$$\frac{\Delta\rho_{ij}}{\rho} = \sum_{k,l} \pi_{ijkl}\sigma_{kl} \tag{4}$$

where i and j denote the directions of the applied current and voltage, while k and l indicate the orientations of the applied stress tensor. The forth-rank piezoresistive coefficient tensor can be collapsed to a second rank tensor (e.g. $\pi_{1111} \rightarrow \pi_{11}$, $\pi_{1122} \rightarrow \pi_{12}$, and $\pi_{2323} \rightarrow \pi_{44}$), using the transformation scheme shown in Table II [53]. The piezoresistive coefficients are used to evaluate the orientation dependence of piezoresistance as well as the magnitude of the effect in arbitrary orientations.

The origin of the piezoresistive effect in semiconductors can be found in the literature including the text books of Doll and Pruitt [53], Bir and Pirkus [54] and Sun *et al.* [55]. Following the first experimental results on the effect of stress on the conductance of silicon and germanium by Smith in 1954 [56], various theoretical studies have been carried out to understand the piezoresistance in semiconductors. The model proposed by Bardeen and Shockley for mobility change in semiconductors subjected to deformation potentials was the basis for most current piezoresistive models [57], including the work of Herring [58] and Herring and Vogt [59], Long [60] and Kanda [61], [62]. The general idea of these models is that, under strain, the energy band structure of semiconductors is modified, resulting in the re-population of the charge carrier in these bands. This leads to the change of carrier effective mass, mobility and consequently conductivity. The explanation for the mechanism of piezoresistance in SiC was also developed based on these models. We will present these theoretical studies in each of the following subsections to make a comparison between experimental and theoretical results.

B. Piezoresistive Effect in Silicon Carbide

Two common methods to characterize the piezoresistive effect in SiC are the bending beam method [68], [73], [89]

This article has been accepted for inclusion in a future issue of this journal. Content is final as presented, with the exception of pagination.

TABLE III
LIST OF GAUGE FACTORS (GF) OF SiC REPORTED IN THE LITERATURE

Polytype	Growing process	Type	Dopant	Carrier concentration (cm^{-3})	GF Room Temp	GF High Temp	Orientation	Stress type
Single 3C-SiC [68]	APCVD	n	Nitrogen	$\sim 10^{18}$	-31.8	-18 (450°C)	[100]	uniaxial
Single 3C-SiC [70]	HMCVD	n	Nitrogen	$\sim 10^{18}$	-27	–	[100]	uniaxial
Single 3C-SiC [71]	APCVD	n	Nitrogen	Unintentionally doped	-18	-7 (400°C)	[100]	biaxial
Single 3C-SiC [77]	LPCVD	n	Nitrogen	$0.4 \sim 2 \times 10^{17}$	-24.8	-11 (450°C)	[100]	biaxial
Single 3C-SiC [91]	APCVD	n	Nitrogen	Highly doped	-16	-12.5 (400°C)	[100]	uniaxial
Single 3C-SiC [73]	LPCVD	p	Aluminum	5×10^{18}	30.3	–	[110]	uniaxial
Single 4H-SiC [89]	–	n	Nitrogen	1.5×10^{19}	20.8	–	(0001) plane	uniaxial
Single 6H-SiC [83]	–	n	Nitrogen	3.8×10^{18}	-29.4	-17 (250°C)	(0001) plane	uniaxial
Single 6H-SiC [84]	–	n	Nitrogen	2×10^{19}	-22	-11 (250°C)	(0001) plane	uniaxial
Single 6H-SiC [84]	–	p	Aluminum	2×10^{19}	27	12 (250°C)	(0001) plane	uniaxial
Poly 3C-SiC [92]	LPCVD	n	Nitrogen	low doped	-10	–	-	biaxial
Poly 3C-SiC [71]	LPCVD	n	Nitrogen	Unintentionally doped	-2.1	–	-	biaxial
Poly 3C-SiC [90]	LPCVD	p	Boron	$10^{18} \sim 10^{20}$	10	7 (200°C)	-	uniaxial
Amorphous SiC [97], [98]	PECVD	n	Nitrogen	-	49	–	-	uniaxial
	Sputtering	n	Nitrogen	-	31	–	-	uniaxial

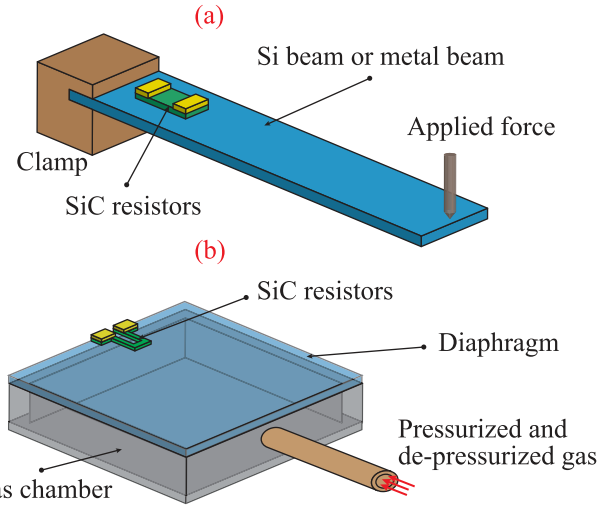

Fig. 2. Experimental setup for characterizing the piezoresistive effect in SiC. (a) Bending beam method. (b) Deforming diaphragm method.

and the deforming diaphragm method [71], [84], as illustrated in Fig. 2. The former method induces a uniaxial strain into the piezoresistive layer, while the latter causes a biaxial strain. In the first method, SiC resistors are patterned or embedded on a substrate which is deflected by a load at the end of the beam to induce a strain on the SiC resistors. In the second method, SiC resistors are formed on a diaphragm structure and the strain is induced by applying a uniform pressure on the diaphragm. When piezoresistors are fabricated at the edge of a diaphragm, the longitudinal strain is much larger than the transverse strain. Therefore the piezoresistive effect in the longitudinal direction is more significant than the transverse direction [69].

A small number of studies on the piezoresistive effect of SiC were reported in the 1970s and 1980s [63]–[65]. However, as the wafers used for characterizing the piezoresistive effect in these studies were related to the Lely process, which was very irregular, these results have not been widely accepted [68]. The first study on the piezoresistive effect in high quality SiC was not reported until the early 90s. Table III shows a summary of the piezoresistive effect of SiC reported in the literature. Several SiC poly types were characterized, including single crystalline α–SiC, β–SiC, poly crystalline and amorphous SiC. In these studies, α–SiC was purchased from Cree [24], where SiC wafers were fabricated using a bulk growth process. The single crystalline β–SiC, poly crystalline, and amorphous SiC films were hetero-epitaxially grown by chemical vapor deposition on other substrates (Si substrate for single crystal SiC, while poly SiC and amorphous SiC can be deposited on several substrates) [68], [70], [77], [92], [97]. Both the piezoresistive effect in n-type and p-type semiconductors was investigated in which the carrier concentration varied from low doping to high doping levels. The n-type SiC was formed using nitrogen, while aluminum and boron were employed to make p-type SiC. At room temperature, the absolute gauge factor of single crystalline SiC is approximately $20 \sim 30$ and decreases to approximately 10 at high temperatures, while the gauge factor of poly crystalline SiC is relatively small compared to single crystalline SiC. Additionally, the data in Table III also indicates that [100] direction has the largest gauge factor in n-type 3C-SiC, whereas [110] orientation has the most significant piezoresistive effect in p-type 3C-SiC. A detailed explanation of the piezoresistive effect in these SiC poly types is presented in the following subsections.

1) The Piezoresistive Effect in Single Crystalline 3C-SiC: Being a preferable crystal for MEMS applications, the piezoresistive effect in 3C-SiC attracts more attention than other poly types [68], [69]. This is due to the fact that, 3C-SiC can be epitaxially grown on large diameter Si wafers [20]. This capability of growth on Si wafers is expected to significantly reduce the cost of 3C-SiC substrates, and makes the

This article has been accepted for inclusion in a future issue of this journal. Content is final as presented, with the exception of pagination.

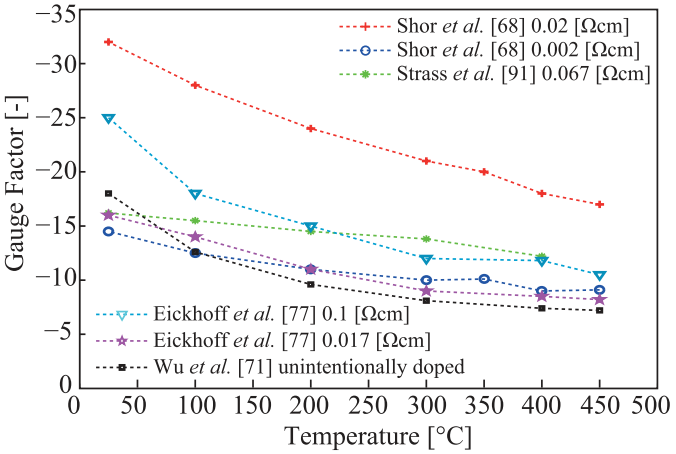

Fig. 3. The temperature dependence of the piezoresistive effect in 3C-SiC. The decrease of the gauge factor with increasing temperature is more pronounced at lower temperature and tends to saturate at high temperatures.

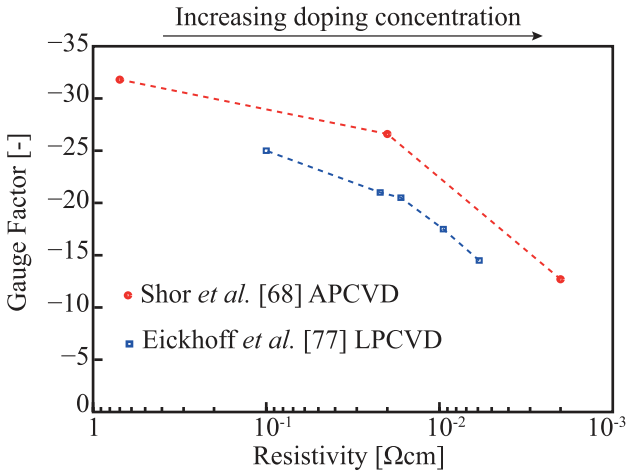

Fig. 4. The doping-level dependence of the piezoresistive effect in 3C-SiC. With the same growth condition (APCVD or LPCVD), the gauge factor decreases with decreasing resistivity (or increasing the doping concentration).

3C-SiC on Si platform more compatible with conventional MEMS processes which have been well established for Si [21], [66], [67].

One of the first systematic studies on the piezoresistive effect in n-type single crystalline 3C-SiC grown on a Si substrate by atmospheric pressure CVD (APCVD) was conducted by Shor *et al.* [68]. At room temperature, the gauge factor of the unintentionally doped 3C-SiC (10^{16} to 10^{17} cm^{-3}) was −31.8. Following the work of Shor *et al.*, a large number of studies were conducted on the piezoresistive effect of 3C-SiC, utilizing different growth processes. As such, the gauge factor of the selective epitaxy growth (SEG) on Si wafer was found to be −18 [69]; Yasui *et al.* reported a gauge factor of −27 in n-type 3C-SiC grown by hot mesh chemical vapor deposition (HM-CVD) [70]. Other groups aimed at transferring/growing 3C-SiC on insulating substrates to prevent the current leakage between SiC and Si layer underneath. Wu *et al.* transferred 3C-SiC onto an insulator (SiO_2/Si) using the fusion bonding technique with a gauge factor of −18 for unintentionally doped samples [71]. Kuo *et al.* proposed a bonding-free method to create SiCOI wafers [72]. The gauge factor of these samples was found to be −17.8. For p-type 3C-SiC, Phan *et al.* recently reported a gauge factor of 30.3 at a carrier concentration of approximately 10^{18} cm^{-3} [73]. This result in p-type 3C-SiC is comparable to that of n-type 3C-SiC in the same range of carrier concentration. The above results show that the piezoresistive effect in 3C-SiC (both n-type and p-type) is ∼3 to 5 times smaller than that of bulk Si (GF ∼ 100), but approximately one order of magnitude larger than most metals (GF = 1 ∼ 2).

As the piezoresistive effect in SiC is aimed at applications used at high temperatures, it is important to investigate the temperature dependence of the piezoresistance in 3C-SiC. To date, only the piezoresistive effect of n-type at high temperatures is available in the literature, while that of p-type has not been reported. The relationship between the gauge factor and temperatures of various studies is plotted in Fig. 3. The gauge factor of n-type 3C-SiC decreases by approximately 50% when temperatures increase from room temperature (23 °C) to above 400 °C. Even though there is a decrease in the piezoresistive effect with increasing temperature, the gauge factor is still at least 5 times larger than that of most metals with a gauge factor of 1 to 2. The large gauge factor of 10 to 18 at approximately 450 °C indicates that SiC has a high sensitivity for mechanical sensing at high temperatures where Si cannot be used [68].

The influence of carrier concentration is of interest for MEMS designers. We plotted the results obtained from the work of Shor *et al.* and Eickhoff *et al.* where the gauge factor was measured against the change of carrier concentration (Fig. 4). It is obvious that the gauge factor decreases with increasing carrier concentration. Additionally, the relationship between the gauge factor and temperature shows that the decrease of the gauge factor in highly doped 3C-SiC at high temperatures (∼20% at 400 °C) is smaller than that of unintentionally doped samples (∼40% at 400 °C). These results indicate that increasing doping concentration could enhance the thermal stability of the gauge factor of 3C-SiC.

The orientation dependence also plays an important role in designing MEMS sensors using the piezoresistive effect. Shor *et al.* [68] and Phan *et al.* [74] characterized the orientation dependence of the n-type and p-type 3C-SiC, respectively. The gauge factor was measured in different directions such as longitudinal [110], transverse [100], and longitudinal [100]. Accordingly, in (100) plane of single crystalline 3C-SiC films, the n-type has the largest gauge factor in [100] direction, while the p-type has the most significant piezoresistive effect in [110] orientation. From these experimental gauge factors in different orientations, we calculated the fundamental piezoresistive coefficients in (100) plane (Table IV).

Figure 5 shows the longitudinal and transverse piezoresistive coefficients in (100) plane. From these values, we can estimate the relative resistance change in an arbitrary orientation in (100) plane using the following equation [53], [62]:

$$\frac{\Delta R}{R} = \pi_l \sigma_l + \pi_t \sigma_t \tag{5}$$

This article has been accepted for inclusion in a future issue of this journal. Content is final as presented, with the exception of pagination.

TABLE IV
THE FUNDAMENTAL PIEZORESISTIVE COEFFICIENTS OF Si AND 3C-SiC

	n Si	p Si	n 3C-SiC	p 3C-SiC
Resistivity [Ωcm]	11.7	7.8	0.7	0.14
π_{11} [$\times 10^{-11}$Pa^{-1}]	**-102.2**	6.6	**-9.6**	1.5
π_{12} [$\times 10^{-11}$Pa^{-1}]	53.4	-1.1	5.8	-1.4
π_{44} [$\times 10^{-11}$Pa^{-1}]	-13.6	**138.1**	1.6	**18.1**

In n-type Si and 3C-SiC, π_{11} is dominant, while π_{44} is largest in p-type.

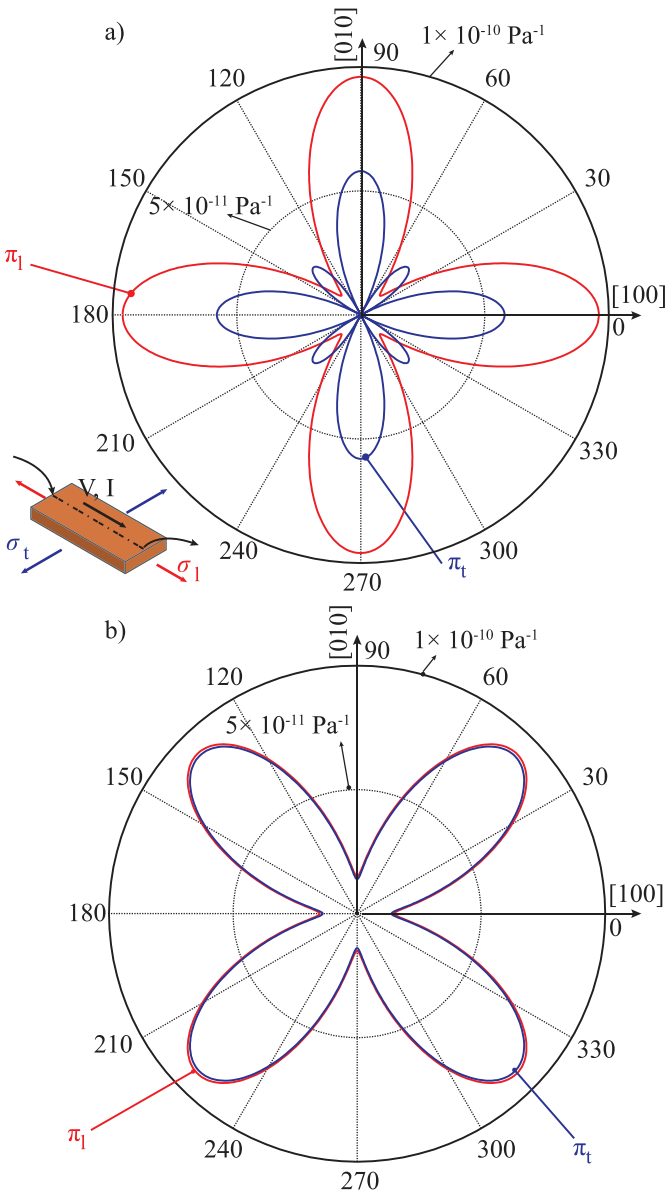

Fig. 5. Piezoresistive coefficients of p-type and n-type 3C-SiC on (100) plane. The piezoresistive coefficients of n-type 3C-SiC were calculated based on the gauge factors reported by Shor *et al.* [68]. For n-type 3C-SiC, the [100] direction possesses the largest piezoresistive effect, whereas in p-type, the [110] direction corresponds to the most significant piezoresistive effect. Reprinted with permission from Phan *et al.* [74]. © American Institute of Physics. (a) n-type single 3C-SiC. (b) p-type single 3C-SiC.

where, π_l and π_t are longitudinal and transverse piezoresistive coefficients; and σ_l and σ_t are longitudinal and transverse stresses, respectively.

Another parameter which needs to be considered is the influence of crystal defects on the piezoresistance of 3C-SiC grown on a Si substrate, since the thermal mismatch and different lattice constants usually lead to the appearance of stacking faults and microtwins at the 3C-SiC/Si interface [75]. These defects degrade the electrical properties of the crystal and therefore could affect the piezoresistance of 3C-SiC [76], [77]. Phan *et al.* reported the thickness dependence of the piezoresistive effect in p-type single crystalline 3C-SiC [78]. The Transmission Electron Microscopy (TEM) images showed that the crystal defects are mainly located at the SiC/Si interface, while their density decreases with increasing the thickness of SiC films. According to the experimental results of Phan *et al.*, under the same growth conditions, the gauge factors were relatively stable for the SiC films with thicknesses above 300 nm (with the difference below 5%). However with films thinner than 150 nm, the gauge factor decreases by more than 20%.

Besides experimental work on the characterizations of the piezoresistive effect in 3C-SiC, theoretical studies have also been carried out, aiming to explain its mechanism. Toriyama and Sugiyama [79], [80] estimated the gauge factor of 3C-SiC based on the electron transport theory by Smith [56] and the deformation potential theory by Herring [58] and Herring Vogt [59] for cubic crystalline semiconductors. There are six equivalent energy minima in the conduction band of 3C-SiC, which are located in [100] equivalent orientation in k-space. Under stress (for instance a compressive stress in [100] direction), the longitudinal valleys in [100] direction shift downwards in energy relative to the four transverse valleys (aligned in [010] and [001] directions). Consequently, electrons transfer from higher energy levels to lower energy levels; and more electrons enter the valley in [100] direction, while fewer electrons distribute in [010] and [001] valleys, Fig. 6 (a). Since the longitudinal mass is greater than the transverse mass, the re-population of electrons under the compressive stress in [100] direction leads to an increase in the resistivity of n-type 3C-SiC. This is consistent with the experimentally observed results, *i.e.* the negative gauge factor of n-type SiC along the principal directions. The longitudinal gauge factor of n-type 3C-SiC can be quantitatively estimated using the following equation [79]:

$$G = 1 + 2\nu - \frac{\Xi_u (L-1)}{3k_B T (2L+1)} (2 + \nu') \frac{F_{-1/2}}{F_{1/2}} \qquad (6)$$

where Ξ_u is an independent constant of the deformation energy, F is the Fermi-Dirac integral, k_B is the Boltzmann constant, $L = \mu_l/\mu_t$ is the ratio of the longitudinal and transverse electron mobilities, and ν and ν' are the Poisson ratio of 3C-SiC and the substrate, respectively. Equation 6 shows that—according to this model—the GF decreases with increasing temperature. Additionally, the Fermi-Dirac integral $F_{-1/2}/F_{1/2}$ is a function of the doping level, indicating the carrier concentration dependence of the piezoresistive effect in SiC. The theoretical results of Toriyama *et al.* show a good agreement with the experimental results reported by Shor *et al.* and Kroetz *et al.* with the carrier concentration in a range of 10^{18} to 10^{20}cm^{-3} (Fig. 6). This indicates that the electron transfer and electron shift mechanisms are valid

This article has been accepted for inclusion in a future issue of this journal. Content is final as presented, with the exception of pagination.

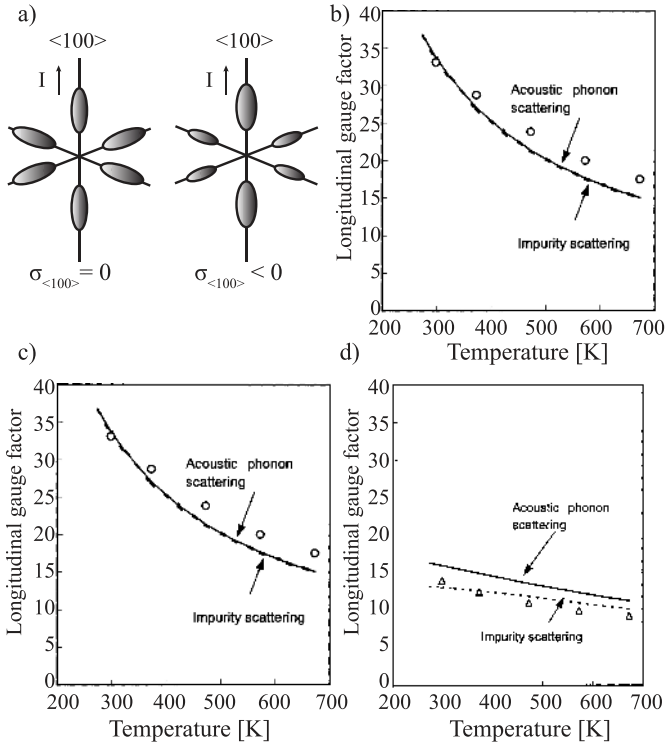

Fig. 6. (a) The first Brillouin zone and carrier re-distribution on the multi-valleys of 3C-SiC conduction band under compressive stress σ_{100}. (b), (c), (d) Numerically calculated longitudinal gauge factor as a function of temperature. Solid and dart lines indicate the theoretical calculation considering acoustic phonon scattering and impurity scattering, respectively, while dot points are experimental data with carrier concentrations of (a) 10^{18} cm^{-3}; (b) 10^{19} cm^{-3}; (c) 10^{20} cm^{-3}; Reprint with permission from [80]. © American Institute of Physics.

for the estimation/explanation of the piezoresistance in n-type 3C-SiC within the above-mentioned range.

For p-type 3C-SiC, unfortunately, there have been no reports on theoretical calculations. This is perhaps due to the complexity of the valance band structure, as in the case of the piezoresistive effect in Si [81], [82]. The piezoresistive effect in p type Si was explained by employing the valence band model of cubic materials. Accordingly, the deformation and warping of the heavy hole and light hole under strain lead to the redistribution of holes in these two bands. The redistribution of holes results in a change in the hole effective mass and thus its mobility, causing a change in electrical conductivity. When a large stress (several GPa) is applied, valence band mixing and decoupling occur [81], leading to the complexity of valence band modification as well as the nonlinear behavior of the piezoresistive effect in Si under large stress regions [82]. It should be noted that the influence of the spin-orbit split-off band in Si was assumed to be negligible due to the large energy level gap from this band to the heavy and light hole bands (0.044 eV). However, in the case of p-type 3C-SiC, the spin-orbit splitting energy at the top of the valence-band is 0.010 eV, which is much smaller than that of Si. Therefore, this band should play an important role in the piezoresistive effect of p-type 3C-SiC.

2) The Piezoresistive Effect in Single Crystalline α-SiC: Although 3C-SiC is more attractive for MEMS devices, several studies on the piezoresistive effect of α-SiC have also been

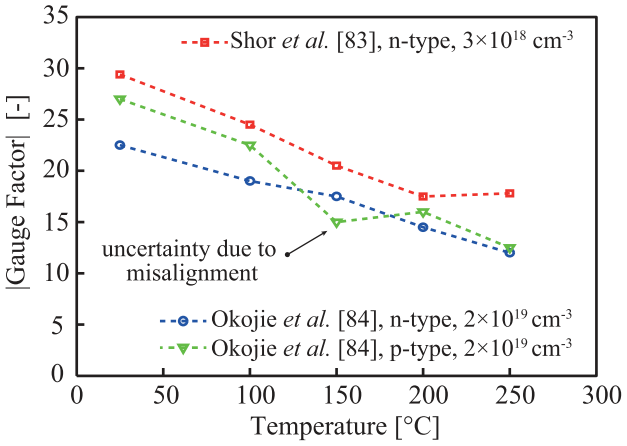

Fig. 7. Gauge factor of 6H-SiC for different temperatures and carrier concentrations.

carried out. This is due to the fact that leakage between SiC/Si is eliminated in the bulk α-SiC wafers.

In most studies on the piezoresistive effect of α-SiC, wafers were sourced from Cree Research Inc. [24]. Low doped n-type 6H-SiC layers which were homo-epitaxially grown on p-type 6H-SiC, were characterized in [83]. The longitudinal GFs of 1.8×10^{17} (low doping) and 3.3×10^{18} (medium doping) for n-type 6H-SiC at room temperature were found to be -35 and -29.4, respectively, which is comparable with that of single crystalline 3C-SiC. The temperature variation between 25 °C and 300 °C causes a reduction in GFs by nearly 40%. The temperature coefficient resistance (TCR) of the low doped and medium doped layers was characterized in a wide range of temperatures, from 25 °C to 600 °C. At temperatures below 100 °C, 6H-SiC has a negative TCR due to the dominance of full carrier ionization, while the TCR becomes positive at temperatures above 100 °C, caused by impurity scattering at high temperatures. These results indicate that the temperature effect is pronounced at both low and medium doping levels.

Okojie *et al.* measured the piezoresistive effect in heavily doped n-type (doping concentration $N_d \approx 2 \times 10^{19}$ cm^{-3}) and p-type (doping concentration $N_a \approx 2 \times 10^{19}$ cm^{-3}) 6H-SiC [84]. For n-type 6H-SiC, the GF was 22 at room temperature, decreasing by about 52% at 250 °C. On the other hand, p-type 6H-SiC has a GF of 27 at room temperature, dropping by approximately 55% at 250 °C (as shown in Fig. 7). The results of Shor *et al.* and Okojie *et al.* clearly show that the gauge factor decreases with increasing carrier concentration. Additionally, even increasing the carrier concentration to 10^{19}cm^{-3}, the gauge factor decreases at almost the same rate as the low doped sample with a concentration of 10^{17}cm^{-3}. Therefore, there is still a lack of evidence to declare that increasing carrier concentration in 6H-SiC could enhance the thermal stability of its piezoresistance.

The electron transfer and mobility shift mechanisms used for piezoresistance analysis of the cubic n type 3C SiC [79] were extended to explain the piezoresistive effect of n-type 6H-SiC [85], [86]. In 6H-SiC, the energy minima are located about halfway between M and L points of the Brillouin zone, leading to the formation of six semi-ellipsoidal valleys.

This article has been accepted for inclusion in a future issue of this journal. Content is final as presented, with the exception of pagination.

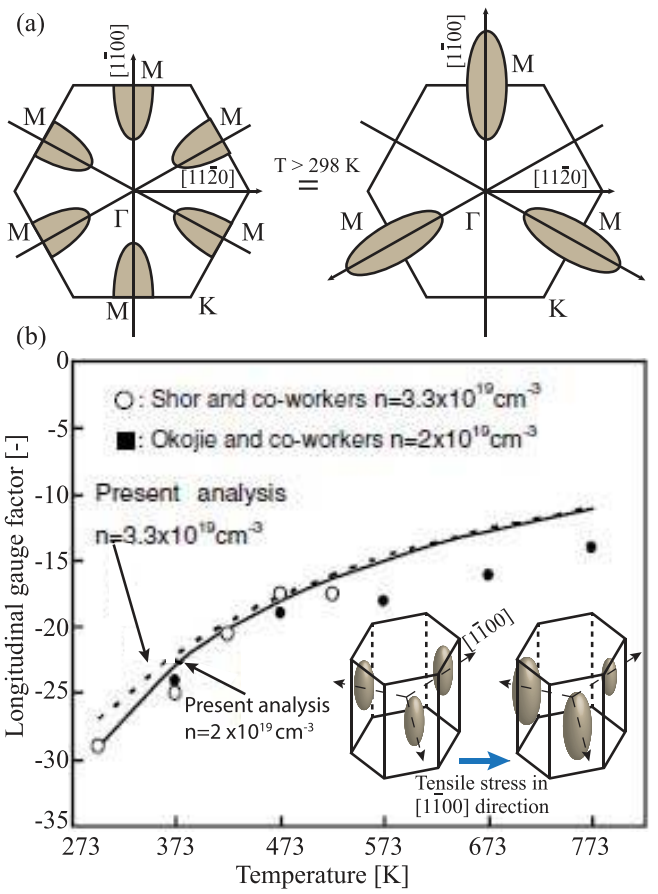

Fig. 8. (a) Six conduction band minima located at M points in the first Brillouin zone (six semi-ellipsoids and equivalent three full ellipsoids), and the re-shape of the energy surfaces of these valleys under stress $\sigma_{1\bar{1}00}$. (b) Comparison of the calculated longitudinal gauge factors and experimental data (n = 2×10^{18}cm^{-3} and 3.3×10^{19}cm^{-3}). Reprint with permission from [86].

The constant energy surface has a double-well-like (or dumb-bell) minimum when the energy level is less than 12 meV and it turns into an ellipsoidal shape with its center being located at M point when the energy level is much larger than 12 meV [87]. As 6H-SiC was characterized at temperatures above 298 K, corresponding to an energy level (3/2 k_BT) above 28 meV, these six semi-ellipsoidal valleys can be approximated as three equivalent full ellipsoids located at M points [87], [88], as illustrated in Fig. 8 (a). When a strain is applied (for instance tensile strain in [1100] direction), a band deformation is induced, thereby breaking the symmetry of the three ellipsoidal valleys, shown in the inset of Fig. 8 (b). As a result, electrons from the higher energy valleys will transfer to the lower energy levels, changing the electron effective mass as well as mobility, and consequently the conductivity of 6H-SiC [86]. The gauge factor was then calculated using the Bir and Pirkus deformation potential theory [54], which found a solid agreement with the experimental results of Shor *et al.* and Okojie *et al.*. Additionally, as the gauge factor obeys 1/T law, Toriyama and Sugiyama suggested that inter-valley scattering has a secondary effect in the piezoresistance of 6H-SiC, while electron transfer and mobility shift could be the origin of the piezoresistive effect in 6H-SiC.

The piezoresistive effect of another common crystalline SiC, 4H-SiC, was reported in [89]. A 1-μm thick n-type 4H-SiC film ($N_d = 1.5 \times 10^{19}$ cm^{-3}) was epitaxially grown on an n-type bulk 4H-SiC substrate. Sandwiched between these layers, a p-type layer ($N_a = 5.4 \times 10^{14}$ cm^{-3}) was grown in order to create a pn junction of 4H-SiC. The transverse GF in this study was reported to be 20.8, which is promising for mechanical sensors. The piezoresistive effect of 4H-SiC at elevated temperatures needs to be evaluated in future work to determine its applicability to high temperature applications.

3) The Piezoresistive Effect in Polycrystalline, Amorphous, and Ceramic SiC: Since polycrystalline and amorphous SiC can be grown on an insulator, these types of SiC-based transducers can be operated at high temperatures without concerns regarding the heterojunction between SiC and Si.

Homma *et al.* grew SiC on SiO_2 using plasma assisted CVD, followed by boron doping (B_2H_6) to form a p-type polycrystalline 3C-SiCOI with the hole concentration between 10^{18} cm^{-3} and 10^{20} cm^{-3} [90]. The GF was about 7 to 10 and had a good stability up to 200 °C.

In contrast to the p-type SiC, more studies were conducted on the piezoresistive effect in polycrystalline n-type 3C-SiC. Strass *et al.* deposited n-type textured and non-textured polycrystalline 3C-SiC films on SiO_2 by LPCVD [91]. Textured polycrystalline 3C-SiC shows an anisotropic piezoresistive effect, with the GF of 10 for the [110] direction and 6.1 for the [100] direction. Whereas, random polycrystalline 3C-SiC shows no directional dependence with the GFs of about 5 in both [110] and [100] directions. The influence of the doping concentration on the piezoresistive effect in n-type polycrystalline 3C-SiC was reported in [92]. The GFs in [100] direction decreased with increasing conductivity from 20 to 120 S/cm. At room temperature, a low conductivity (low doped polycrystalline 3C-SiC) shows a larger GF of about −9.5, while a high conductivity (highly doped polycrystalline 3C-SiC) has a GF of about −6. The data reported in the literature infers that polycrystalline 3C-SiC has a lower piezoresistive effect than single crystalline 3C-SiC. This phenomenon was also reported to occur in Si, in which the piezoresistive effect of polycrystalline Si is smaller than that of single crystalline silicon [93]. The decrease of the piezoresistance in poly SiC compared to crystalline SiC can be explained by using the model of polycrystalline semiconductors. Accordingly, the diminution of gauge factor could be reasoned by the random alignment of crystal grain inside the poly materials [94], or due to the scattering of carriers at grain boundaries [95], [96].

Fraga *et al.* investigated the piezoresistive effect in amorphous SiC [97], [98]. Two methods of PECVD (Plasma Enhanced CVD) and radio frequency magnetron sputtering were used to grow amorphous SiC on a SiO_2/Si substrate. Nitrogen gas was used for *in situ* doping to form n-type amorphous SiC. The longitudinal GFs of the amorphous SiC were in the range from 31 to 49. The TCR of amorphous SiC was approximately 31 to 45 ppm/°C, indicating the thermal stability of amorphous SiC grown on a glass substrate. However, the authors did not report on the behavior of the piezoresistive effect at high temperatures.

This article has been accepted for inclusion in a future issue of this journal. Content is final as presented, with the exception of pagination.

TABLE V
PIEZORESISTIVE EFFECT OF SiC NANO STRUCTURES

Authors	Poly type	Diameter [nm]	Gauge factor
Shao *et al.* [106]	3C-SiC	150	-6.9
Zeng *et al.* [107]	3C-SiC	320	14.1
Bi *et al.* [108]	3C-SiC	230	4.5 to 46.2
Gao *et al.* [109]	6H-SiC	170	25.6 to 79
Nakamura [111]	-	3 (thickness)	20 to 60

Thus, additional investigation must be carried out to evaluate the piezoresistance of amorphous SiC at elevated temperatures.

The piezoresistive effect in ceramic SiC was also reported. Kishimoto *et al.* characterized ceramic 6H-SiC, doped with aluminum, boron, and gallium [99], [100]. The piezoresistive coefficients of Al doped and Ga doped ceramic 6H-SiC films were about 20×10^{-11} Pa^{-1} and 30×10^{-11} Pa^{-1}, respectively, which is comparable with p-type and n-type 3C-SiC. The B doped samples had a relatively large piezoresistive coefficient of 60×10^{-11} Pa^{-1}, approximately half of the value for single crystalline Si.

4) The Piezoresistive Effect in SiC Nanowires and Nano Thin Films: Recently, SiC nanowires and nano thin films have attracted significant attention from the research community since they combine the excellent physical properties of SiC material and the advantages of the low dimension structures (1-D in nanowires and 2-D in nano thin films) [101]–[103]. A giant piezoresistive effect with a GF of 5000 was reported in silicon nanowires (Si NWs) [104], which is hypothesized to be caused by the modification of surface charge redistribution due to the external stresses [52], [105]. These impressive results obtained in Si NWs have become a motivation for the research of the piezoresistive effect in SiC nano structures for harsh environment applications [111]. Table V lists the work on the piezoresistance of SiC nanostructures reported in the literature.

Most studies on the piezoresistive effect of SiC NWs used the bottom up method to grow nanowires [106]–[109]. Shao *et al.* [106] and Zeng *et al.* [107] applied mechanical stress to 3C-SiC NWs by using piezoelectric and electrostatic actuators and measured the induced strain by SEM. The gauge factors reported by Shao *et al.* and Zeng *et al.* were -6.9 and 14.1 respectively, which is 2 to 4 times smaller than that of bulk 3C-SiC.

Bi *et al.* used a different approach to investigate the piezoresistive effect of 3C-SiC NWs, in which an AFM tip was pressed against a 3C-SiC nanowire placed on a metallic graphite substrate [108]. The transverse gauge factor of the nanowire was found to be 4.5 to 46.2. Besides the band structure change of SiC NWs due to strain, Bi *et al.* suggested that changed surface states in SiC NWs may also contribute to their piezoresistance. The SiC NWs would be oxidized during the growth process or when exposed to air, forming a Si-O outer layer [108]. The external stress could change the surface states, leading to a change of the built-in potential near the nanowire surface. This built-in potential would mediate the concentration and mobility, and as a consequence would change the conductance of the nanowires.

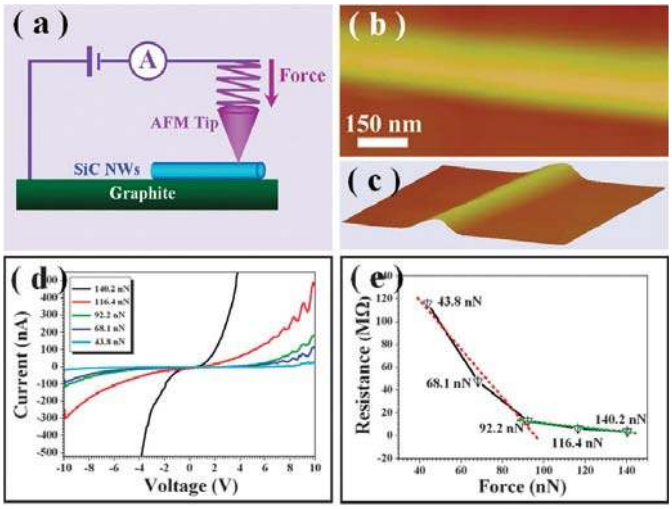

Fig. 9. (a) Schematic of the electromechanical characterization measurement; (b) and (c) AFM and topography images of a single 6H-SiC nanowire lying on a graphite substrate, respectively; (d) IV curves recorded at different applied forces across the nanowire; (e) relationship between the resistance of the nanowire and the applied force. Reprint with permission from [109].

Another experimental study was conducted by Gao *et al.*, characterizing the piezoresistive effect of p-type 6H-SiC NWs, Fig. 9 [109]. The piezoresistive coefficient in p-type 6H-SiC was relatively large, in the range of 51.2 to 159.5×10^{-11} Pa^{-1}, compared to that of 18.1×10^{-11} Pa^{-1} in bulk 3C-SiC. This is perhaps the largest piezoresistive coefficient reported in SiC material to date. However, it should be pointed out that the Young's modulus of the characterized 6H-SiC NWs was relatively small ($\sim$50 GPa) [109], which is at least 6 times smaller than that of bulk SiC. Thus the gauge factor of the characterized 6H-SiC was calculated to be in a range of 25.6 to 79, which cannot be considered as a giant piezoresistive effect. Thus, unlike the case of Si NWs, there has been no report on the giant piezoresistive effect in SiC NWs to date. A number of studies have been carried out to theoretically investigate the influence of scale on the piezoresistive effect of SiC nano structures [110], [111]. Nakamura *et al.* simulated the piezoresistive effect in n-type α and β-SiC (0001) nanosheets with a thickness of 3 nm based on the density functional theory [111]–[113]. The simulation results show that at room temperature the gauge factor of SiC nano thin films is in the range of 30 to 60, and decrease approximately 50% at 500 °C (Fig. 10). This theoretical study based on the first principle calculation suggests that the piezoresistive effect of nano thin films is comparable to that of bulk SiC wafer, and no giant piezoresistive effect is predicted based on the quantum confinement. In the numerical simulation of Nakamura *et al.*, the electrostatic depletion in nanowires and nano thin films when reducing the doping concentration, which was deployed to explain the giant piezoresistive effect in Si [52], [114], [115], was not taken into account.

C. Applications of Silicon Carbide Piezoresistive Effect

Along with the characterization of the fundamental properties of SiC, several applications of the SiC piezoresistive effect have been demonstrated.

This article has been accepted for inclusion in a future issue of this journal. Content is final as presented, with the exception of pagination.

TABLE VI
LIST OF SiC PIEZORESISTIVE EFFECT BASED PRESSURE SENSORS

Authors	Poly type	Substrate	Sensitivity		Released method
			Room Temperature (25°C)	High Temperatures	
Shor *et al.* [68]	Single 3C-SiC	SiO_2/Steel	8.7 [μV/V_{bias}]/kPa	4.4 [μV/V_{bias}]/kPa (350°C)	-
Eickhoff *et al.* [69]	Single 3C-SiC	SOI	35 [μV/V_{bias}]/kPa	21[μV/V_{bias}]/kPa (200°C)	ICP etching
Wu *et al.* [71]	Single 3C-SiC	SiO_2	25.8 [μV/V_{bias}]/kPa	9.2 [μV/V_{bias}]/kPa (400°C)	KOH
Ziermann *et al.* [116], [118]	Single 3C-SiC	SOI	20 [μV/V_{bias}]/kPa	11 [μV/V_{bias}]/kPa (300°C)	ICP etching
Berg *et al.* [117]*	Single 3C-SiC	SOI	0.8 [μV/V_{bias}]/kPa	0.5 [μV/V_{bias}]/kPa (300°C)	-
Fraga *et al.* [97]	Amorphous SiC	SiO_2	48 [μV/V_{bias}]/kPa	–	KOH
Chung [119]	Poly 3C-SiC	SiO_2	1 [μV/V_{bias}]/kPa	0.25 [μV/V_{bias}]/kPa (400°C)	RIE
Wieczorek *et al.* [120]*	6H-SiC	Bulk SiC	0.2 [μV/V_{bias}]/kPa	0.13 [μV/V_{bias}]/kPa (400°C)	Ultrasonic Drilling
Okojie *et al.* [84], [121]	6H-SiC	Bulk SiC	1.2 [μV/V_{bias}]/kPa	0.6 [μV/V_{bias}]/kPa (500°C)	Electrochemical etching
Okojie *et al.* [122]	4H-SiC	Bulk SiC	1.74 [μV/V_{bias}]/kPa	0.7 [μV/V_{bias}]/kPa (600°C)	–
Okojie [123]	4H-SiC	Bulk SiC	2.9 [μV/V_{bias}]/kPa	3.4 [μV/V_{bias}]/kPa (800°C)	RIE
Akiyama *et al.* [130]	4H-SiC	Bulk SiC	2.6 [μV/V_{bias}]/kPa	–	Mechanical milling

* The sensitivity of the pressure sensors was calculated from the output voltage at a constant applied current.

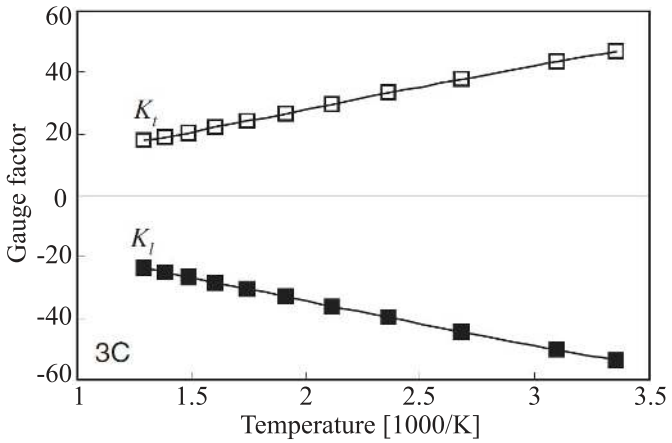

Fig. 10. Calculated longitudinal and transverse gauge factors in [100] orientation of n-type 3C-SiC nano thin films at a carrier concentration of 10^{19} cm^{-3}. Reprint with permission from [111].

One of the most important applications of the piezoresistive effect in SiC is pressure sensing in combustion chambers of engines at high temperatures [116]–[123]. Table VI lists the pressure sensors reported in the literature with their general concept shown in Fig. 11. Various poly types such as 3C, 4H, 6H-SiC, and amorphous SiC pressure sensors were deployed, where different techniques were utilized to form the diaphragm of piezoresistive pressure sensors. For instance, for SiC on SiO_2/Si or SOI substrates [124]–[126], the Si layer at the bottom was etched using wet etching (KOH) or dry etching (RIE, ICP) [21]. For bulk SiC wafers, the bottom SiC layer can also be thinned down using electrochemical etching or RIE. However, as the etching rate of SiC is very low (100 nm to 1 μm/min [127], [128]) in comparison to that of Si (10 μm/min [129]), laser micro-machining and wafer drilling/milling are employed to reduce the etching time of SiC [120], [130]. For further reading on the fabrication process of SiC MEMS devices, we recommend the review paper of Zorman and Parro [131] and the book of Saddow [132].

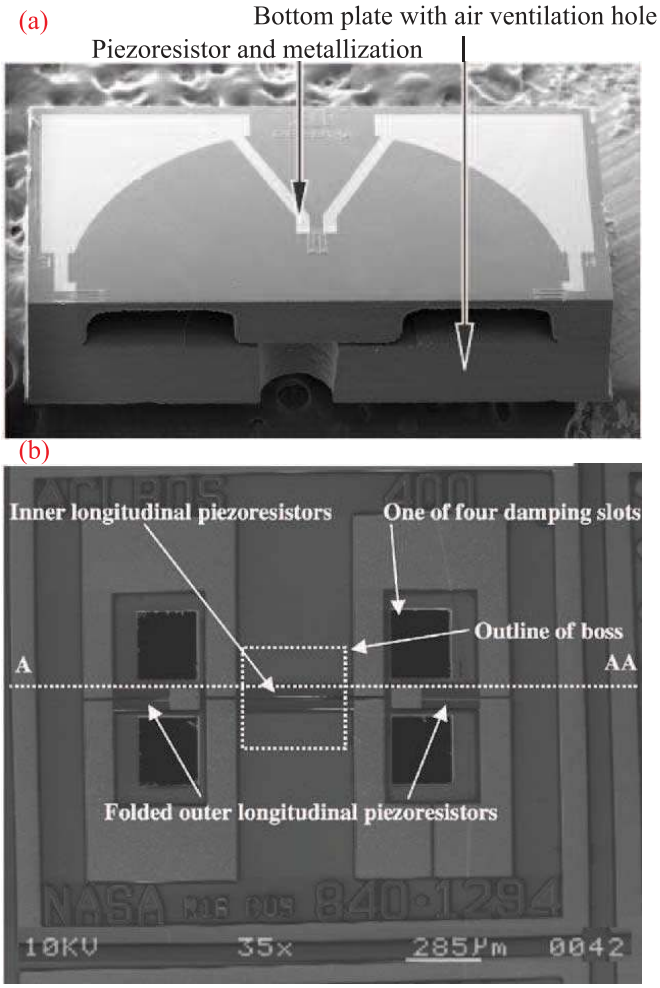

Fig. 11. Concept of SiC piezoresistive based sensors: (a) Pressure sensor. (b) Accelerometer. Reprint with permission from [121] and [134].

It can also be seen in Table VI that the sensitivity of sensors at room temperatures varied from several hundreds [nV/V_{bias}]/kPa to several tens [μV/V_{bias}]/kPa, depending on

This article has been accepted for inclusion in a future issue of this journal. Content is final as presented, with the exception of pagination.

the thickness and diameter of diaphragms, as well as the Young's modulus of the substrates. The sensitivity of pressure sensors decreased at high temperature due to the decrease of the gauge factor of SiC at elevated temperatures, as presented in the previous section.

Most of the work on the development of SiC based pressure sensors was performed as a proof of concept of the feasibility of using the piezoresistive effect in SiC for pressure monitoring at high temperatures. However, the investigation of the resolution, noise level and reliability of these pressure sensors was rarely conducted. Okojie *et al.* measured the offset voltage of 4H-SiC pressure sensors during 1000 hours-test at 600 °C [122]. The experimental results showed that the agglomeration of metal (Au) on SiC could lead to a large deviation of offset voltage (92 mV). The same authors also characterized the performance of 4H-SiC based sensors at 800 °C. Unlike the properties of the piezoresistive effect in SiC, being that its gauge factors decrease with increasing temperatures, the output of the 4H-SiC pressure sensors developed by Okojie *et al.* decreased from room temperature to 400 °C, and then increased at temperatures above 400 °C [123]. Although the authors suggested the modification of band structure under stress at high temperatures and the packaging process could lead to an increase of sensitivity, it remains unclear which mechanism is the main reason causing this phenomenon.

Besides the applications at high temperatures, SiC is expected to be utilized in high shock and high frequency devices due to the large ratio of Young's modulus to mass density in comparison to that of Si. 6H-SiC accelerometers with a capability of measuring extreme impacts of up to 40,000 g were reported [133]. The accelerometers had 6H-SiC piezoresistors patterned on a diaphragm as sensing elements, and a proof mass on the back side (Fig. 11 (b)). The accelerometers were designed in several shapes with the first resonant frequencies ranging from 200 to 800 kHz. The sensitivities of the accelerometers were in the range of 40 to 250 nV/g, demonstrating the applicability of piezoresistive effect in SiC for high shock and high frequency transducers.

The piezoresistive effect of SiC is also valuable for monitoring the strain of hot sections inside combustion chambers. Fraga *et al.* proposed amorphous SiC strain sensors which have a relative resistance change of 4.8% per 1 ppm of strain at room temperature [134].

IV. Conclusions and Future Prospects

Various studies on the characterization of the piezoresistive effect in SiC and the development of SiC sensors have been carried out. Large GFs at both room temperature ($|GF| \approx 30$) and high temperature ($|GF| \approx 10$ to 18) demonstrate the potential of the piezoresistance in SiC for mechanical sensing devices. It should be noted that the gauge factor of SiC decreases with increasing temperature [80], [86], [110], and that SiC has a temperature coefficient of gauge factor (TCGF) comparable to that of Si [62], [68], [84]. However, the piezoresistive effect of SiC can be utilized in niche applications where Si cannot be used, such as corrosive and oxidizing environments of jet engines [12] or high temperature conditions of combustion chambers [20]. The recent development of SiC pressure sensors operating at temperatures above 500 °C has demonstrated the feasibility of using the piezoresistive effect in SiC for harsh environments such as in engines [117], [121], [123]. Additionally, SiC based mechanical sensors can also be well integrated with all-SiC based circuits which are expected to replace Si based electronic devices in harsh environments (e.g. high power density and high temperature) [50]. Furthermore, because of the excellent stiffness and chemical inertness of SiC, studies on the piezoresistive effect in SiC could extend beyond electronic devices operating at high temperatures to cover high-frequency [42] and bio applications [44]. For instance, utilizing the large GFs of SiC at room temperature could make the development of SiC based self-sensing high-Q-factor/ high-frequency resonators possible, and thereby may eliminate the need for optical measurements [135]. On the other hand, the piezoresistance of SiC can also be employed to characterize the mechanical properties of cells [136], [137].

The experimental results and theoretical studies reported in literature could give valuable hints for MEMS designers in employing the piezoresistive effect of SiC such as orientation dependence as well as the dependence on the carrier concentration and temperature. However, to fully understand the piezoresistive effect in SiC and its applications, various questions still need to be addressed. In most studies on the piezoresistive effect, the induced stress was relatively small (in order of several hundred MPa), and behaviors of the piezoresistive effect in large stress ranges (several GPa) has not been investigated. Additionally, the piezoresistive effect of α-SiC and amorphous SiC has not been fully understood. For instance, the characterized temperatures of α-SiC are relatively low ($\sim$250 °C), and the orientation dependence of this poly type has not been investigated. Furthermore, SiC MEMS fabrication and packaging processes still faces several challenges. As such, due to the extremely high chemical stability of SiC, the etching rate of bulk SiC is relatively low (200 nm/min to 1 μm/min), resulting in a time-consuming etching process to create MEMS movable structures [131]. Alternative methods such as wafer milling and laser machining have been proposed; however structures fabricated by these methods normally have large feature size and poor surface roughness [130]. In addition, at high temperature, thermal expansion causes de-bonding, deformation, and cracking in devices [123], as well as the metal agglomeration could induce signal drift [122], [123]. Therefore, further investigation of above-mentioned issues is required to bring SiC piezoresistive sensors from research to practical applications or commercialization.

Research on nanowire-based sensors has attracted a great deal of interest recently. Unlike Si nanowires, no giant piezoresistive effect in SiC has been reported until now. It should be noted that the diameter of the characterized nanowires is relatively large (above 150 nm). Additionally, in most of the previous studies the influence of carrier concentration, and orientation dependence of SiC nanowires have not been mentioned. Furthermore, to date, only

This article has been accepted for inclusion in a future issue of this journal. Content is final as presented, with the exception of pagination.

bottom-up grown SiC nanowires have been preliminary investigated, while the piezoresistive effect in top-down machined SiC nanowires has not been reported. Since the top-down technique is more compatible with MEMS fabrication processes, the properties of top-down nanowires should be investigated in detail to enable the future development of nanoscale sensing transducers. Additionally, as the giant piezoresistive effect has been observed in Si nanowires field effect transistors (FET) [138], [139], it is also interesting to characterize the role of gate voltage on the piezoresistance of SiC nanowire based FET.

ACKNOWLEDGMENT

This work was performed in part at the Queensland node of the Australian National Fabrication Facility, a company established under the National Collaborative Research Infrastructure Strategy to provide nano and micro-fabrication facilities for Australia's researchers. The authors thank Dr. Nicholas Dahl and Dr. Melissa Heath for proofreading the manuscript.

REFERENCES

[1] A. A. Barlian, W.-T. Park, J. R. Mallon, Jr., A. J. Rastegar, and B. L. Pruitt, "Review: Semiconductor piezoresistance for microsystems," *Proc. IEEE*, vol. 97, no. 3, pp. 513–552, Mar. 2009.

[2] W. P. Eaton and J. H. Smith, "Micromachined pressure sensors: Review and recent developments," *Proc. SPIE—Int. Soc. Opt. Eng.*, vol. 3046, pp. 30–41, 1997.

[3] S. S. Kumar and B. D. Pant, "Design principles and considerations for the 'ideal' silicon piezoresistive pressure sensor: A focused review," *Microsyst. Technol.*, vol. 20, no. 7, pp. 1213–1247, Jul. 2014.

[4] M. Elwenspoek and H. V. Jansen, *Silicon Micromachining*. Cambridge, U.K.: Cambridge Univ. Press, Aug. 2004.

[5] D. V. Dao, K. Nakamura, T. T. Bui, and S. Sugiyama, "Micro/nano-mechanical sensors and actuators based on SOI-MEMS technology," *Adv. Natural Sci, Nanosci. Nanotechnol.*, vol. 1, no. 1, p. 013001, 2010.

[6] S. M. Spearing, "Materials issues in microelectromechanical systems (MEMS)," *Acta Mater.*, vol. 48, no. 1, p. 179–196, Jan. 2000.

[7] D. V. Dao, T. Toriyama, J. Wells, and S. Sugiyama, "Six-degree of freedom micro force-moment sensor for application in geophysics," in *Proc. IEEE 15th Int. Conf. Micro Electro Mech. Syst. (MEMS)*, Las Vegas, NV, USA, Jan. 2002, pp. 312–315.

[8] H. Yousef, M. Boukallel, and K. Althoefer, "Tactile sensing for dexterous in-hand manipulation in robotics—A review," *Sens. Actuators A, Phys.*, vol. 167, no. 2, pp. 171–187, Jun. 2011.

[9] N. Minh-Dung, P. Hoang-Phuong, K. Matsumoto, and I. Shimoyama, "A sensitive liquid-cantilever diaphragm for pressure sensor," in *Proc. IEEE 26th Int. Conf. Micro Electro Mech. Syst. (MEMS)*, Jan. 2013, pp. 617–620.

[10] N.-C. Tsai and C.-Y. Sue, "Review of MEMS-based drug delivery and dosing systems," *Sens. Actuators A, Phys.*, vol. 134, no. 2, pp. 555–564, Mar. 2007.

[11] M. Li, H. X. Tang, and M. L. Roukes, "Ultra-sensitive NEMS-based cantilevers for sensing, scanned probe and very high-frequency applications," *Nature Nanotechnol.*, vol. 2, no. 2, pp. 114–120, 2007.

[12] D. G. Senesky, B. Jamshidi, K. B. Cheng, and A. P. Pisano, "Harsh environment silicon carbide sensors for health and performance monitoring of aerospace systems: A review," *IEEE Sensors J.*, vol. 9, no. 11, pp. 1472–1478, Nov. 2009.

[13] V. C. Gungor and G. P. Hancke, "Industrial wireless sensor networks: Challenges, design principles, and technical approaches," *IEEE Trans. Ind. Electron.*, vol. 56, no. 10, pp. 4258–4265, Oct. 2009.

[14] M. Werner *et al.*, "High—Temperature sensors based on SiC and diamond technology," *Sensors Update*, vol. 5, no. 1, pp. 141–190, Apr. 1999.

[15] G. H. Kroetz, M. H. Eickhoff, and H. Moeller, "Silicon compatible materials for harsh environment sensors," *Sens. Actuators A, Phys.*, vol. 74, nos. 1–3, pp. 182–189, Apr. 1999.

[16] M. Willander, M. Friesel, Q.-U. Wahab, and B. Straumal, "Silicon carbide and diamond for high temperature device applications," *J. Mater. Sci. Mater. Electron.*, vol. 17, no. 1, pp. 1–25, Jan. 2006.

[17] W. R. Fahrner, R. Job, and M. Werner, "Sensors and smart electronics in harsh environment applications," *Microsyst. Technol.*, vol. 7, no. 4, pp. 138–144, Nov. 2001.

[18] P. G. Neudeck, R. S. Okojie, and L.-Y. Chen, "High-temperature electronics—A role for wide bandgap semiconductors?" *Proc. IEEE*, vol. 90, no. 6, pp. 1065–1076, Jun. 2002.

[19] M. R. Werner and W. R. Fahrner, "Review on materials, microsensors, systems and devices for high-temperature and harsh-environment applications," *IEEE Trans. Ind. Electron.*, vol. 48, no. 2, pp. 249–257, Apr. 2001.

[20] M. Mehregany, C. A. Zorman, N. Rajan, and C. H. Wu, "Silicon carbide MEMS for harsh environments," *Proc. IEEE*, vol. 86, no. 8, pp. 1594–1609, Aug. 1998.

[21] P. M. Sarro, "Silicon carbide as a new MEMS technology," *Sens. Actuators A, Phys.*, vol. 82, nos. 1–3, pp. 210–218, May 2000.

[22] D. Massé, "Market for GaN and SiC semiconductors set to rise 18x from 2012 to 2022," *J. Microw.*, vol. 56, no. 6, p. 55, 2013.

[23] L. Wang *et al.*, "Growth of 3C–SiC on 150-mm Si(100) substrates by alternating supply epitaxy at 1000 °C," *Thin Solid Films*, vol. 519, no. 19, pp. 6443–6446, Jul. 2011.

[24] Cree Inc., Durham, NC, USA. (2014). *CREE Materials Catalogue: Silicon Carbide Substrates 2014*. [Online]. Available: http://www.cree.com

[25] R. Maboudian, C. Carraro, D. G. Senesky, and C. S. Roper, "Advances in silicon carbide science and technology at the micro- and nanoscales," *J. Vac. Sci. Technol. A*, vol. 31, no. 5, p. 050805, 2013.

[26] W. D. Edwards and R. P. Beaulieu, "Germanium piezoresistive element on a flexible substrate," *J. Phys. E, Sci. Instrum.*, vol. 2, no. 7, pp. 613–615, 1969.

[27] A. D. Bykhovski, V. V. Kaminski, M. S. Shur, Q. C. Chen, and M. A. Khan, "Piezoresistive effect in wurtzite *n*-type GaN," *Appl. Phys. Lett.*, vol. 68, no. 6, p. 818, 1996.

[28] V. Tilak, A. Vertiatchikh, J. Jiang, N. Reeves, and S. Dasgupta, "Piezoresistive and piezoelectric effects in GaN," *Phys. Status Solidi C*, vol. 3, no. 6, pp. 2307–2311, Jun. 2006.

[29] C. H. Park, B.-H. Cheong, K.-H. Lee, and K. J. Chang, "Structural and electronic properties of cubic, 2H, 4H, and 6H SiC," *Phys. Rev. B*, vol. 49, no. 7, pp. 4485–4493, 1994.

[30] J. B. Casady and R. W. Johnson, "Status of silicon carbide (SiC) as a wide-bandgap semiconductor for high-temperature applications: A review," *Solid-State Electron.*, vol. 39, no. 10, pp. 1409–1422, Oct. 1996.

[31] V. Cimalla, J. Pezoldt, and O. Ambacher, "Group III nitride and SiC based MEMS and NEMS: Materials properties, technology and applications," *J. Phys. D, Appl. Phys.*, vol. 40, no. 20, p. 6386, 2007.

[32] M. Wijesundara and R. Azevedo, *Silicon Carbide Microsystems for Harsh Environments*. New York, NY, USA: Springer, 2011.

[33] Q. Zhang, R. Callanan, M. K. Das, S.-H. Ryu, A. K. Agarwal, and J. W. Palmour, "SiC power devices for microgrids," *IEEE. Trans. Power Electron.*, vol. 25, no. 12, pp. 2889–2896, Dec. 2010.

[34] P. Friedrichs, "SiC power devices as enabler for high power density—Aspects and prospects," *Mater. Sci. Forum*, vols. 778–780, pp. 1104–1109, Feb. 2014.

[35] G.-S. Chung and J.-M. Jeong, "Fabrication of micro heaters on polycrystalline 3C-SiC suspended membranes for gas sensors and their characteristics," *Microelectron. Eng.*, vol. 87, no. 11, pp. 2348–2352, Nov. 2010.

[36] J.-G. Lee, M. I. Lei, S.-P. Lee, S. Rajgopal, and M. Mehregany, "Micro flow sensor using polycrystalline silicon carbide," *J. Sensor Sci. Technol.*, vol. 18, no. 2, pp. 147–153, 2009.

[37] T. Dinh *et al.*, "Charge transport and activation energy of amorphous silicon carbide thin film on quartz at elevated temperature," *Appl. Phys. Exp.*, vol. 8, no. 6, p. 061303, 2015.

[38] S. Ma, S. Wang, F. Iacopi, and H. Huang, "A resonant method for determining the residual stress and elastic modulus of a thin film," *Appl. Phys. Lett.*, vol. 103, no. 3, p. 031603, 2013.

[39] G. Cheng, T.-H. Chang, Q. Qin, H. Huang, and Y. Zhu, "Mechanical properties of silicon carbide nanowires: Effect of size-dependent defect density," *Nano Lett.*, vol. 14, no. 2, pp. 754–758, 2014.

[40] S. Gong, N.-K. Kuo, and G. Piazza, "GHz high-Q lateral overmoded bulk acoustic-wave resonators using epitaxial SiC thin film," *J. Micromech. Syst.*, vol. 21, no. 2, pp. 253–255, Apr. 2012.

This article has been accepted for inclusion in a future issue of this journal. Content is final as presented, with the exception of pagination.

[41] A. R. Kermany, G. Brawley, N. Mishra, E. Sheridan, W. P. Bowen, and F. Iacopi, "Microresonators with *Q*-factors over a million from highly stressed epitaxial silicon carbide on silicon," *Appl. Phys. Lett.*, vol. 104, no. 8, p. 081901, 2014.

[42] Z. Wang, J. Lee, and P. X.-L. Feng, "Spatial mapping of multimode Brownian motions in high-frequency silicon carbide microdisk resonators," *Nature Commun.*, vol. 5, p. 5158, Nov. 2014.

[43] C. Förster *et al.*, "Group III-nitride and SiC based micro- and nano-electromechanical resonators for sensor applications," *Phys. Status Solidi A*, vol. 203, no. 7, pp. 1829–1833, May 2006.

[44] A. Oliveros, A. Guiseppi-Elie, and S. E. Saddow, "Silicon carbide: A versatile material for biosensor applications," *Biomed. Microdevices*, vol. 15, no. 2, pp. 353–368, Apr. 2013.

[45] S. E. Saddow *et al.*, "Single-crystal silicon carbide: A biocompatible and hemocompatible semiconductor for advanced biomedical applications," *Matter. Sci. Forum*, vols. 679–680, pp. 824–830, Mar. 2011.

[46] G. Gabriel *et al.*, "Manufacturing and full characterization of silicon carbide-based multi-sensor micro-probes for biomedical applications," *Microelectron. J.*, vol. 38, no. 3, pp. 406–415, Mar. 2007.

[47] S. Fujita, "Wide-bandgap semiconductor materials: For their full bloom," *Jpn. J. Appl. Phys.*, vol. 54, no. 3, p. 030101, 2015.

[48] H. Amano, "Progress and prospect of the growth of wide-band-gap group III nitrides: Development of the growth method for single-crystal bulk GaN," *J. Jpn. Appl. Phys.*, vol. 52, no. 5R, p. 050001, 2013.

[49] N. G. Wright and A. B. Horsfall, "SiC sensors: A review," *J. Phys. D, Appl. Phys.*, vol. 40, no. 20, pp. 6345–6354, 2007.

[50] C.-M. Zetterling, "Integrated circuits in silicon carbide for high-temperature applications," *MRS Bull.*, vol. 40, no. 5, pp. 431–438, May 2015.

[51] N. G. Wright, A. B. Horsfall, and K. Vassilevski, "Prospects for SiC electronics and sensors," *Mater. Today*, vol. 11, nos. 1–2, pp. 16–21, Jan./Feb. 2008.

[52] A. C. H. Rowe, "Piezoresistance in silicon and its nanostructures," *J. Mater. Res.*, vol. 29, no. 6, pp. 731–744, 2014.

[53] J. C. Doll and B. L. Pruitt, *Piezoresistor Design and Applications*, 1st ed. New York, NY, USA: Springer, 2013.

[54] G. L. Bir and G. E. Pikus, *Symmetry and Strain-Induced Effects in Semiconductors*. Hoboken, NJ, USA: Wiley, Jan. 1974.

[55] Y. Sun, S. E. Thompson, and T. Nishida, *Strain Effect in Semiconductors: Theory and Device Applications*. 1st ed. New York, NY, USA: Springer, 2009.

[56] C. S. Smith, "Piezoresistance effect in germanium and silicon," *Phys. Rev.*, vol. 94, pp. 42–49, Apr. 1954.

[57] J. Bardeen and W. Shockley, "Deformation potentials and mobilities in non-polar crystals," *Phys. Rev.*, vol. 80, pp. 72–80, Oct. 1950.

[58] C. Herring, "Transport properties of a many-valley semiconductor," *Bell Syst. Tech. J.*, vol. 34, no. 2, pp. 237–290, Mar. 1955.

[59] C. Herring and E. Vogt, "Transport and deformation-potential theory for many-valley semiconductors with anisotropic scattering," *Phys. Rev.*, vol. 101, no. 3, pp. 944–961, Feb. 1956.

[60] D. Long, "Stress dependence of the piezoresistance effect," *J. Appl. Phys.*, vol. 32, no. 10, pp. 2050–2051, 1961.

[61] Y. Kanda, "Piezoresistance effect of silicon," *Sens. Actuators A, Phys.*, vol. 28, no. 2, pp. 83–91, Jul. 1991.

[62] Y. Kanda and Y. Kanda, "A graphical representation of the piezoresistance coefficients in silicon," *IEEE Trans. Electron Devices*, vol. 29, no. 1, pp. 64–70, Jan. 1982.

[63] I. V. Rapatskaya, G. E. Rudashevskii, M. G. Kasaganova, M. I. Islitsin, M. B. Reifman, and E. F. Fedotova, "Piezoresistance coefficients of n-type α-SiC," *Soviet Phys. Solid State*, vol. 9, no. 12, p. 2833, 1968.

[64] G. N. Guk, N. Y. Usol'tseva, V. S. Shadrin, and N. K. Prokop'eva, "The piezoresistance of cubic SiC under hydrostatic compression," *Sov. Phys. Semicond.*, vol. 10, pp. 83–84, 1976.

[65] G. N. Guk, V. M. Lyubimskii, E. P. Gofman, V. B. Zinovev, and E. A. Chalyi, "Temperature dependence of the piezoresistive effect constant π_{11} of n-type SiC(6H)," *Soviet Phys. Semicond.*, vol. 9, p. 104, 1974.

[66] A. Qamar *et al.*, "The dependence of offset voltage in p-type 3C-SiC van der Pauw device on applied strain," *IEEE Electron Device Lett.*, vol. 36, no. 7, pp. 708–710, Jul. 2015.

[67] H.-P. Phan *et al.*, "Orientation dependence of the pseudo-Hall effect in p-type 3C–SiC four-terminal devices under mechanical stress," *RSC Adv.*, vol. 5, no. 69, pp. 56377–56381, 2015.

[68] J. S. Shor, D. Goldstein, and A. D. Kurtz, "Characterization of n-type β-SiC as a piezoresistor," *IEEE Trans. Electron Devices*, vol. 40, no. 6, pp. 1093–1099, Jun. 1993.

[69] M. Eickhoff, H. Möller, G. Kroetz, J. V. Berg, and R. Ziermann, "A high temperature pressure sensor prepared by selective deposition of cubic silicon carbide on SOI substrates," *Sens. Actuators A, Phys.*, vol. 74, nos. 1–3, pp. 56–59, Apr. 1999.

[70] K. Yasui, H. Miura, M. Takata, and T. Akahane, "SiCOI structure fabricated by catalytic chemical vapor deposition," *Thin Solid Film*, vol. 516, no. 5, pp. 644–647, Jan. 2008.

[71] C.-H. Wu, C. A. Zorman, and M. Mehregany, "Fabrication and testing of bulk micromachined silicon carbide piezoresistive pressure sensors for high temperature applications," *IEEE Sensors J.*, vol. 6, no. 2, pp. 316–324, Apr. 2006.

[72] H.-I. Kuo, C. A. Zorman, and M. Mehregany, "Fabrication and testing of single crystalline 3C-SiC devices using a novel SiC-on-insulator substrate," in *Proc. 12th Int. Conf. Solid-State Sens., Actuators, Microsyst. (TRANSDUCERS)*, Boston, MA, USA, Jun. 2003, pp. 742–745.

[73] H.-P. Phan *et al.*, "Piezoresistive effect of p-type single crystalline 3C-SiC thin film," *IEEE Electron Device Lett.*, vol. 35, no. 3, pp. 399–401, Mar. 2014.

[74] H.-P. Phan *et al.*, "Fundamental piezoresistive coefficients of p-type single crystalline 3C-SiC," *Appl. Phys. Lett.*, vol. 104, no. 11, p. 111905, 2014.

[75] W. M. Vetter and M. Dudley, "Characterization of defects in 3C-silicon carbide crystals," *J. Crystal Growth*, vol. 260, nos. 1–2, pp. 201–208, Jan. 2004.

[76] M. Eickhoff, H. Möller, J. Stoemenos, S. Zappe, G. Kroetz, and M. Stutzmann, "Influence of crystal quality on the electronic properties of n-type 3C-SiC grown by low temperature low pressure chemical vapor deposition," *J. Appl. Phys.*, vol. 95, no. 12, p. 7908, 2004.

[77] M. Eickhoff and M. Stutzmann, "Influence of crystal defects on the piezoresistive properties of 3C–SiC," *J. Appl. Phys.*, vol. 96, no. 5, p. 2878, 2004.

[78] H.-P. Phan *et al.*, "Thickness dependence of the piezoresistive effect in p-type single crystalline 3C-SiC nanothin films," *J. Mater. Chem. C*, vol. 2, no. 35, pp. 7176–7179, 2014.

[79] T. Toriyama and S. Sugiyama, "Analysis of the piezoresistive effect in n-type β-SiC based on electron transport and deformation potential theory," in *Proc. Int. Symp. Micromechatron. Human Sci. (MHS)*, Oct. 2000, pp. 175–180.

[80] T. Toriyama and S. Sugiyama, "Analysis of piezoresistance in n-type β-SiC for high-temperature mechanical sensors," *Appl. Phys. Lett.*, vol. 81, no. 15, p. 2797, 2002.

[81] K. Suzuki, H. Hasegawa, and Y. Kanda, "Origin of the linear and nonlinear piezoresistance effects in p-type silicon," *Jpn. J. Appl. Phys.*, vol. 23, no. 11A, p. L871, 1984.

[82] J. S. Milne, I. Favorskiy, A. C. H. Rowe, S. Arscott, and C. Renner, "Piezoresistance in silicon at uniaxial compressive stresses up to 3 GPa," *Phys. Rev. Lett.*, vol. 108, no. 25, p. 256801, Jun. 2012.

[83] J. S. Shor, L. Bemis, and A. D. Kurtz, "Characterization of monolithic n-type 6H-SiC piezoresistive sensing elements," *IEEE Trans. Electron Devices*, vol. 41, no. 5, pp. 661–665, May 1994.

[84] R. S. Okojie, A. A. Ned, A. D. Kurtz, and W. N. Carr, "Characterization of highly doped n- and p-type 6H-SiC piezoresistors," *IEEE Trans. Electron Devices*, vol. 45, no. 4, pp. 785–790, Apr. 1998.

[85] T. Toriyama and S. Sugiyama, "Analysis of piezoresistance in n-type 6H SiC for high-temperature mechanical sensors," in *Proc. 12th Int. Conf. Solid-State Sens., Actuators, Microsyst. (TRANSDUCERS)*, Boston, MA, USA, Jun. 2003, pp. 758–761.

[86] T. Toriyama, "Piezoresistance consideration on n-type 6H SiC for MEMS-based piezoresistance sensors," *J. Micromech. Microeng.*, vol. 14, no. 11, pp. 1445–1448, 2004.

[87] T. Kinoshita, K. M. Itoh, M. Schadt, and G. Pensl, "Theory of the electron mobility in *n*-type 6H-SiC," *J. Appl. Phys.*, vol. 85, no. 12, pp. 8193–8198, 1999.

[88] W. J. Choyke, H. Matsunami, and G. Pensl, *Silicon Carbide: Recent Major Advances*. New York, NY, USA: Springer, 2004, pp. 441–443.

[89] T. Akiyama, D. Briand, and N. F. de Rooij, "Design-dependent gauge factors of highly doped n-type 4H-SiC piezoresistors," *J. Micromech. Microeng.*, vol. 22, no. 8, p. 085034, 2012.

[90] T. Homma, K. Kamimura, H. Y. Cai, and Y. Onuma, "Preparation of polycrystalline SiC films for sensors used at high temperature," *Sens. Actuators A, Phys.*, vol. 40, no. 2, pp. 93–96, Feb. 1994.

This article has been accepted for inclusion in a future issue of this journal. Content is final as presented, with the exception of pagination.

[91] J. Strass, M. Eickhoff, and G. Kroetz, "The influence of crystal quality on the piezoresistive effect of β-SiC between RT and 450 °C measured by using microstructures," in *Proc. Int. Conf. Solid-State Sens. Actuators (TRANSDUCERS)*, Chicago, IL, USA, Jun. 1997, pp. 1439–1442.

[92] M. Eickhoff, M. Möller, G. Kroetz, and M. Stutzmann, "Piezoresistive properties of single crystalline, polycrystalline, and nanocrystalline n-type 3C-SiC," *J. Appl. Phys.*, vol. 96, no. 5, pp. 2872–2877, 2004.

[93] J. Y. W. Seto, "Piezoresistive properties of polycrystalline silicon," *J. Appl. Phys.*, vol. 47, no. 11, p. 4780, 1976.

[94] H.-P. Phan *et al.*, "The effect of strain on the electrical conductance of p-type nanocrystalline silicon carbide thin films," *J. Mater. Chem. C*, vol. 3, no. 6, pp. 1172–1176, 2015.

[95] X. Liu, C. Shi, and R. Chuai, *Polycrystalline Silicon Piezoresistive Nano Thin Film Technology*. Rijeka, Croatia: InTech, 2010. ISBN: 978-953-307-045-2.

[96] V. Mosser, J. Suski, J. Goss, and E. Obermeier, "Piezoresistive pressure sensors based on polycrystalline silicon," *Sens. Actuators A, Phys.*, vol. 28, no. 2, pp. 113–132, Jul. 1991.

[97] M. A. Fraga, M. Massi, H. Furlan, I. C. Oliveira, L. A. Rasia, and C. F. R. Mateus, "Preliminary evaluation of the influence of the temperature on the performance of a piezoresistive pressure sensor based on a-SiC film," *Microsyst. Technol.*, vol. 17, no. 3, pp. 477–480, Mar. 2011.

[98] M. A. Fraga, H. Furlan, R. S. Pessoa, L. A. Rasia, and C. F. R. Mateus, "Studies on SiC, DLC and TiO_2 thin films as piezoresistive sensor materials for high temperature application," *Microsyst. Technol.*, vol. 18, nos. 7–8, pp. 1027–1033, Aug. 2012.

[99] A. Kishimoto, D. Mutaguchi, H. Hayashi, and Y. Numata, "High temperature piezoresistance properties of 6H-SiC ceramics doped with trivalent elements," *Mater. Sci. Eng. B*, vol. 135, no. 2, pp. 145–149, 2006.

[100] A. Kishimoto, Y. Okada, and H. Hayashi, "Improvement of the piezoresistive effect properties of silicon carbide ceramics through co-doping of aluminum nitride and nitrogen," *Ceram. Int.*, vol. 34, no. 4, pp. 845–848, May 2008.

[101] K. Zekentes and K. Rogdakis, "SiC nanowires: Material and devices," *J. Phys. D, Appl. Phys.*, vol. 44, no. 13, p. 133001, 2011.

[102] R. Wu, K. Zhou, C. Y. Yue, J. Wei, and Y. Pan, "Recent progress in synthesis, properties and potential applications of SiC nanomaterials," *Prog. Mater. Sci.*, vol. 72, pp. 1–60, Jul. 2015.

[103] A. Lugstein, M. Steinmair, A. Steiger, H. Kosina, and E. Bertagnolli, "Anomalous piezoresistance effect in ultrastrained silicon nanowires," *Nano Lett.*, vol. 10, no. 8, pp. 3204–3208, 2010.

[104] R. He and P. Yang, "Giant piezoresistance effect in silicon nanowires," *Nature Nanotechnol.*, vol. 1, pp. 42–46, Oct. 2006.

[105] A. C. H. Rowe, "Silicon nanowires feel the pinch," *Nature Nanotechnol.*, vol. 3, no. 6, pp. 311–312, 2008.

[106] R. Shao, K. Zheng, Y. Zhang, Y. Li, Z. Zhang, and X. Han, "Piezoresistance behaviors of ultra-strained SiC nanowires," *Appl. Phys. Lett.*, vol. 101, no. 23, p. 233109, 2012.

[107] H. Zeng, T. Li, M. Bartenwerfer, S. Fatikow, and Y. Wang, "*In situ* SEM electromechanical characterization of nanowire using an electrostatic tensile device," *J. Phys. D, Appl. Phys.*, vol. 46, no. 30, p. 305501, 2013.

[108] J. Bi *et al.*, "Highly sensitive piezoresistance behaviors of n-type 3C-SiC nanowires," *J. Mater. Chem. C*, vol. 1, no. 30, pp. 4514–4517, 2013.

[109] F. Gao, J. Zheng, M. Wang, G. Wei, and W. Yang, "Piezoresistance behaviors of p-type 6H-SiC nanowires," *Chem. Commun.*, vol. 47, no. 43, pp. 11993–11995, 2011.

[110] K. Nakamura, T. Toriyama, and S. Sugiyama, "Analysis on piezoresistive property of silicon carbide on the basis of first-principles calculation," in *Proc. 27th Sensor Symp. Sensors, Micromach., Appl.Syst.*, Oct. 2010, pp. 1–6.

[111] K. Nakamura, T. Toriyama, and S. Sugiyama, "First-principles simulation on piezoresistivity in alpha and beta silicon carbide nanosheets," *Jpn. J. Appl. Phys.*, vol. 50, no. 6S, p. 06GE05, 2011.

[112] K. Nakamura, Y. Isono, and T. Toriyama, "First-principles study on piezoresistance effect in silicon nanowires," *Jpn. J. Appl. Phys.*, vol. 47, no. 6S, pp. 5132–5138, 2008.

[113] K. Nakamura, Y. Isono, T. Toriyama, and S. Sugiyama, "Simulation of piezoresistivity in n-type single-crystal silicon on the basis of the first-principles band structure," *Phys. Rev. B*, vol. 80, p. 045205, Jul. 2009.

[114] Y. Yang and X. Li, "Giant piezoresistance of p-type nano-thick silicon induced by interface electron trapping instead of 2D quantum confinement," *Nanotechnology*, vol. 22, no. 1, p. 015501, 2011.

[115] L. M. Terman, "An investigation of surface states at a silicon/silicon oxide interface employing metal-oxide-silicon diodes," *Solid-State Electron.*, vol. 5, no. 5, pp. 285–299, Sep./Oct. 1962.

[116] R. Ziermann, J. von Berg, W. Reichert, E. Obermeier, M. Eickhoff, and G. Krotz, "A high temperature pressure sensor with β-SiC piezoresistors on SOI substrates," in *Proc. Int. Conf. Solid-State Sens. Actuators (TRANSDUCERS)*, Chicago, IL, USA, Jun. 1997, pp. 1411–1414.

[117] J. von Berg, R. Ziermann, W. Reichert, and E. Obermeier, "Measurement of the cylinder pressure in combustion engines with a piezoresistive β-SiC-on-SOI pressure sensor," in *Proc. 4th Int. High Temp. Electron. Conf.*, Jun. 1998, pp. 245–249.

[118] R. Ziermann *et al.*, "High temperature piezoresistive β-SiC-on-SOI pressure sensor with on chip SiC thermistor," *Mater. Sci. Eng. B*, vols. 61–62, pp. 576–578, Jul. 1999.

[119] G. S. Chung, "Fabrication and characterization of a polycrystalline 3C-SiC piezoresistive micro-pressure sensor," *J. Korean Phys. Soc.*, vol. 56, no. 6, pp. 1759–1762, 2010.

[120] G. Wieczorek, B. Schellin, E. Obermeier, G. Fagnani, and L. Drera, "SiC based pressure sensor for high-temperature environments," in *Proc. IEEE Sensors Conf.*, Oct. 2007, pp. 748–751.

[121] R. S. Okojie, A. A. Ned, and A. D. Kurtz, "Operation of α(6H)-SiC pressure sensor at 500 °C," *Sens. Actuators A, Phys.*, vol. 66, nos. 1–3, pp. 200–204, Apr. 1998.

[122] R. S. Okojie, D. Lukco, C. Blaha, V. Nguyen, and E. Savrun, "Zero offset drift suppression in SiC pressure sensors at 600 °C," in *Proc. IEEE Sensors Conf.*, Nov. 2010, pp. 2269–2274.

[123] R. S. Okojie, D. Lukco, V. Nguyen, and E. Savrun, "4H-SiC piezoresistive pressure sensors at 800 °C with observed sensitivity recovery," *IEEE Electron Device Lett.*, vol. 36, no. 2, pp. 174–176, Feb. 2015.

[124] A. Sandhu and S. Jinno, "Piezoresistive properties of 3C-SiC films anodically bonded to aluminosilicate glass substrates," *Electron. Lett.*, vol. 36, no. 6, pp. 497–498, Mar. 2000.

[125] W. Reichert, E. Obermeier, and J. Stoemenos, "β-SiC films on SOI substrates for high temperature applications," *Diamond Rel. Mater.*, vol. 6, no. 10, pp. 1448–1450, Aug. 1997.

[126] G.-S. Chung and R. Maboudian, "Bonding characteristics of 3C-SiC wafers with hydrofluoric acid for high-temperature MEMS applications," *Sens. Actuators A, Phys.*, vol. 119, no. 2, pp. 599–604, Apr. 2005.

[127] T. K. Hossain, S. MacLaren, J. M. Engel, C. Liu, I. Adesida, and R. S. Okojie, "The fabrication of suspended micromechanical structures from bulk 6H-SiC using an ICP-RIE system," *J. Micromech. Microeng.*, vol. 16, no. 4, pp. 751–756, 2006.

[128] S. Tanaka, K. Rajanna, T. Abe, and M. Esashi, "Deep reactive ion etching of silicon carbide," *J. Vac. Sci. Technol. B*, vol. 19, no. 6, pp. 2173–2176, 2001.

[129] F. Laermer and A. Urban, "Challenges, developments and applications of silicon deep reactive ion etching," *Microelectron. Eng.*, vols. 67–68, pp. 349–355, Jun. 2003.

[130] T. Akiyama, D. Briand, and N. F. de Rooij, "Piezoresistive n-type 4H-SiC pressure sensor with membrane formed by mechanical milling," in *Proc. IEEE Sensors Conf.*, Oct. 2011, pp. 222–225.

[131] C. A. Zorman and R. J. Parro, "Micro- and nanomechanical structures for silicon carbide MEMS and NEMS," *Phys. Status Solidi B*, vol. 245, no. 7, pp. 1404–1424, Jul. 2008.

[132] S. Saddow, *Silicon Carbide Biotechnology: A Biocompatible Semiconductor for Advanced Biomedical Devices and Applications*. Upper Saddle River, NJ, USA: Elsevier, 2011.

[133] A. R. Atwell, R. S. Okojie, K. T. Kornegay, S. L. Roberson, and A. Beliveau, "Simulation, fabrication and testing of bulk micromachined 6H-SiC high-g piezoresistive accelerometers," *Sens. Actuators A, Phys.*, vol. 104, no. 1, pp. 11–18, Mar. 2003.

[134] M. A. Fraga, H. Furlan, S. M. Wakavaiachi, and M. Massi, "Fabrication and characterization of piezoresistive strain sensors for high temperature applications," in *Proc. IEEE Int. Conf. Ind. Technol. (ICIT)*, Mar. 2010, pp. 513–516.

[135] M. Kumar and H. Bhaskaran, "Ultrasensitive room-temperature piezoresistive transduction in graphene-based nanoelectromechanical systems," *Nano Lett.*, vol. 15, no. 4, pp. 2562–2567, 2015.

[136] J. Polesel-Maris *et al.*, "Piezoresistive cantilever array for life sciences applications," *J. Phys., Conf. Ser.*, vol. 61, no. 1, p. 955, 2007.

[137] G. Shekhawat, S.-H. Tark, and V. P. Dravid, "MOSFET-embedded microcantilevers for measuring deflection in biomolecular sensors," *Science*, vol. 311, no. 5767, pp. 1592–1595, 2006.

This article has been accepted for inclusion in a future issue of this journal. Content is final as presented, with the exception of pagination.

[138] T.-K. Kang, "Evidence for giant piezoresistance effect in n-type silicon nanowire field-effect transistors," *Appl. Phys. Lett.*, vol. 100, no. 16, p. 163501, 2012.
[139] P. Neuzil, C. C. Wong, and J. Reboud, "Electrically controlled giant piezoresistance in silicon nanowires," *Nano Lett.*, vol. 10, no. 4, pp. 1248–1252, Mar. 2010.

Hoang-Phuong Phan received the B.Eng. and M.Eng. degrees from the University of Tokyo, Japan, in 2011 and 2013, respectively. He is currently pursuing the PhD. degree with the Queensland Micro- and Nanotechnology Centre, Griffith University, Australia. His research interests include microelectromechanical systems (MEMS), advanced materials, physics of semiconductors, and nanotechnologies. His current studies are characterizing the electrical and mechanical properties of SiC, and developing SiC-based MEMS sensors used in harsh environments. He received the Japanese Government Scholarship for undergraduate and post-graduate studies from 2006 to 2013. He is a recipient of the Griffith University Postgraduate Research Scholarship and the International Postgraduate Research Scholarship.

Dzung Viet Dao received the Ph.D. degree in microelectromechanical systems (MEMS) from Ritsumeikan University, Japan, in 2003. He was with Ritsumeikan University, Japan, as a Postdoctoral Research Fellow from 2003 to 2006, a Lecturer from 2006 to 2007, and the Chair Professor from 2007 to 2011. Since 2011, he has been with Griffith University as a Senior Lecturer with the School of Engineering, where he is currently teaching mechatronics and mechanical engineering. Since 2013, he has served as a Member of the National Committee on Mechatronics Engineers, Australia. He has authored over 250 papers in scientific journals and conference proceedings, and holds 15 Japanese patents. He is a Member of the Queensland Micro and Nanotechnology Centre. His current research interests include nanostructures, MEMS sensors and actuators, silicon carbide transducers for harsh environment, and mechatronics.

Koichi Nakamura received the B.Eng., M.Eng., and Ph.D. degrees from Kyoto University, in 1994, 1996, and 2000, respectively, all in molecular engineering. From 1999 to 2006, he was with Kyoto University. In 2006, he relocated to Ritsumeikan University and was a Chair Professor with the Research Institute for Nanomachine System Technology, Ritsumeikan University, from 2009 to 2011. Since 2011, he has been an Associate Professor with the Center for the Promotion of Interdisciplinary Education and Research, Kyoto University. He also works as an Associate Professor with the Department of Materials Science and Engineering, Egypt-Japan University of Science and Technology, Egypt.

Sima Dimitrijev (S'87–M'88–SM'01) received the B.Eng., M.Sc., and Ph.D. degrees in electronics engineering from the University of Nis, Nis, Yugoslavia, in 1982, 1985, and 1989, respectively. He is currently a Professor with the School of Engineering, Griffith University, and the Deputy Director of the Queensland Micro- and Nanotechnology Centre. He has authored the book *Principles of Semiconductor Devices—Second Edition* (Oxford University Press, 2011).

Nam-Trung Nguyen received the Dip.-Ing., Dr.Ing., and Dr.Ing.Habil. degrees from the Chemnitz University of Technology, Germany, in 1993, 1997, and 2004, respectively. In 1998, he was a Postdoctoral Research Engineer with the University of California at Berkeley, USA. From 1999 to 2013, he was an Associate Professor with Nanyang Technological University, Singapore. Since 2013, he has served as a Professor and the Director of the Queensland Micro- and Nanotechnology Centre with Griffith University, Australia.

View publication stats